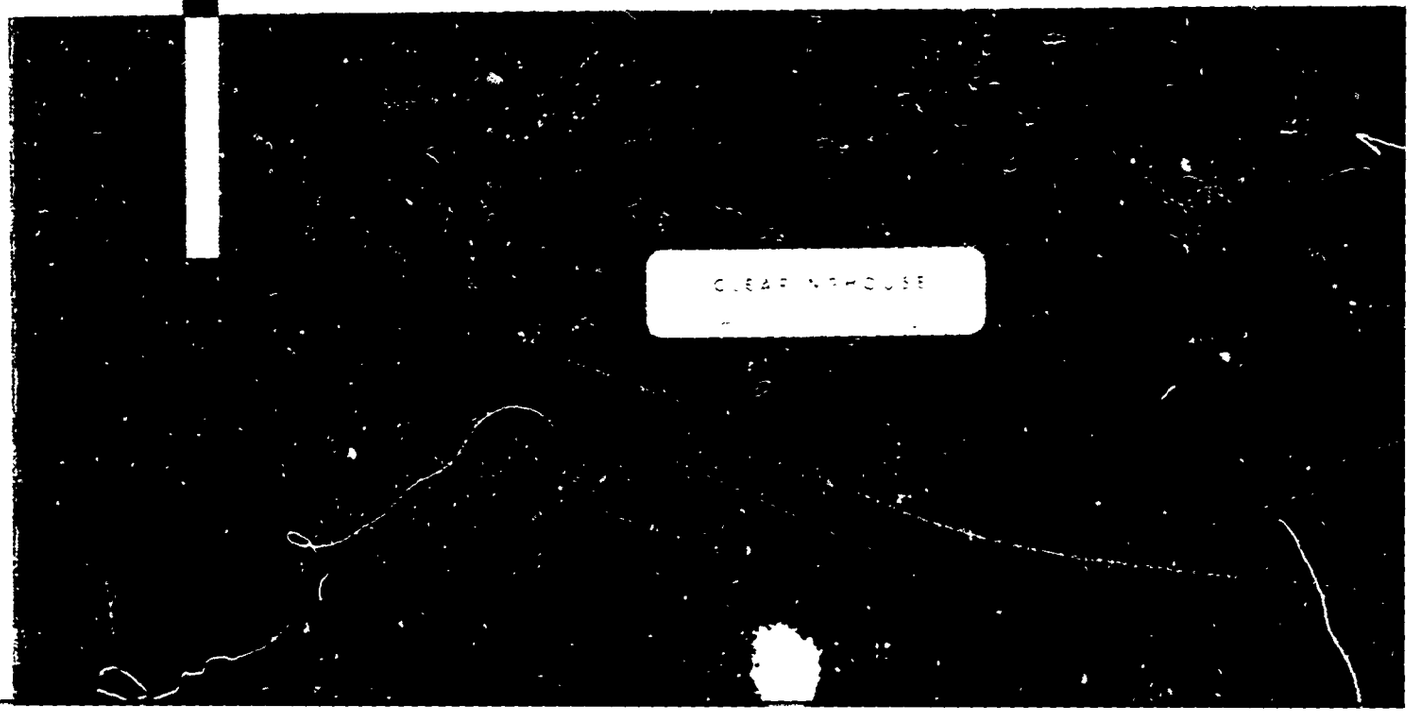

Contract DOT-CG-83851A

AN EXPERIMENTAL STUDY TO DETERMINE THE MOTIONS AND MOORING TENSIONS OF THREE BUOYS

Final Technical Report

27 December 1968 LMSC/D022460

Approved: R. L. Waid, Manager
Hydrodynamics, 57-25
Ocean Systems Engineering

Prepared: Dr. W. C. Webster
Hydrodynamics, 57-25
Ocean Systems Engineering

SUMMARY

Models of three buoys were tested in the Lockheed Underwater Missile Facility (LUMF). In these tests, the effects of both waves and currents were simulated. Two buoys were models of ones already in service, one was a model of a buoy currently under development. As a result of the tests, a single-point mooring configuration for the new, CANUN buoy was developed.

Of particular interest during this study was the visibility of the buoys in various sea and current conditions. The test results were used to predict the fraction of time that the buoys remained within 2°, 3° and 4° of vertical. Over all current conditions and sea states the CANUN with the new, single-point moor remained most vertical.

TABLE OF CONTENTS

Section 1

INTRODUCTION

There are currently several different types of navigational buoys used by the Coast Guard. Several of the locations in which these buoys are used have severe environments including wind, waves, currents and combinations of these conditions. In addition to the forces exerted by the environment on the buoys, the seawater itself causes considerable damage by corrosion and erosion. In order to survive these diffucult surroundings, the current buoys are all rather large and heavy structures. The steel hull material and the large on board power supply (batteries) require frequent inspection to assure their proper performance.

The primary purpose of a navigational buoy is, of course, to mark the boundaries of areas of safe passage. In order for this marking to be effective the buoy must be visible at a significant distance. Buoys often have a light, bell, horn, radar reflector or a combination of these to provide additional identifiers for nighttime, fog or other conditions for which direct visibility is impaired. For most purposes, the light and radar reflector are the most desirable, since the sound from horns or bells is not very directional, and can be reflected by other objects. This is particularly true for larger vessels which may never sail close enough to distinquish the exact direction of a bell or horn signal. For a light or radar reflector to be effective, it must be within the line of sight of the viewer. Further, if the beam of the light or the reflection pattern of the radar reflector are very narrow-banded (as is required for long distance visibility) then the buoy must remain substantially upright for it to be seen.

Either large static pitch and roll angles or large pitch and roll motions can prevent a light on the buoy from being visible. For instance, if a buoy light has a static pitch angle of 10° and its light has a 4° beam, then it will be essentially ineffective as a marker on a clear night. Similarly, if the roll and pitch motions are out of phase, the buoy is never upright and this may also lead to difficult visibility problems. No method now exists to predict the behavior of these buoys and to assess their visibility characteristics in various environmental situations.

Another severe problem is that of buoy placement. The buoys are connected to an anchor by means of a chain which is generally two or three times the local depth of water. During periods of high waves or currents, it is possible for the chain tension to move the anchor, or perhaps even to break the chain. It is important, therefore to know the magnitudes of the maximum chain tension in order to size both the chain and anchor. Again, no method for predicting these limiting forces exists.

At present, the Coast Guard is undertaking the development of a new class of buoys which may eventually replace all of the older types. The new buoy, called the CANUN, is manufactured of fiberglass, spun to form a strong, lightweight and corrosion resistant hull. New compact batteries and the fiberglass lead to a buoy significantly smaller and lighter than the current buoys. It is possible that the small size and reliability of these new buoys will have a dramatic effect on the maintenance schedule as well as the ships used as buoy tenders.

The experimental program reported herein was aimed at determining the attitude, the motions and the mooring tensions of three types of buoys for representative ranges of currents and ocean waves. The first two

buoy types, called the 1CR and 8x26 represent two common types now in use. A third was the CANUN buoy, mentioned above. The objective of this study is to determine not only the relative merits of these buoys but to determine the absolute effect of these motions on the visibility of the buoys under realistic sea conditions.

Section 2

THE BUOYS

Schematic diagrams of the three buoy configurations are shown in Figures 1, 2 and 3. A brief description of each follows:

2.1 1CR BUOY

The 1CR buoy (Figure 1) has a cylindrical hull shape with a truncated cone on the bottom. The bottom of the conical portion contains internal weights which provide stability for the buoy. The superstructure of the buoy consists of lightweight vertical steel plates arranged in a cross-shaped pattern and above these plates a light is mounted. The plates act as optical markers during daylight and as radar reflectors. The buoy is arranged so that it can be moored in several locations. For mooring, there is an eye at the bottom and a current bar on the side of the conical portion. The bar has several holes to which a mooring chain can be attached. In waters of little current the buoy is moored at the bottom eye; in locations of moderate to severe current, the buoy is moored on the current bar. The lower holes correspond to smaller currents, the upper ones to larger currents.

2.2 8x26 BUOY

The 8x26 buoy (Figure 2) is essentially a large diameter cylindrical shape. The bottom of the cylinder is a spherical dome, and the top is flat with access ports for its internal batteries. Connected to the bottom of the buoy is a cylindrical rod and a heavy counterweight for stability. The superstructure is much like the 1CR with reflectors and a light. The buoy is moored with a bridal arrangement attached

to two large eyes on opposite sides of the bottom of the dome. A wood chafing strip is mounted on the rod supporting the counterweight to protect it from the eye connecting the bridal to the mooring chain. No changes in location of the moor are made for various currents.

2.3 CANUN BUOY

The CANUN buoy (Figure 3). This new type of buoy is rather narrower than the above two buoys. Its hull is a truncated cone shape with a cylindrical portion on the bottom. The cylindrical portion contains counterweights sufficient for stability of the buoy. The superstructure is also conical in form with a light at its truncated top. Inside the superstructure a radar reflector array will be mounted. The original buoy configuration included a mooring eye at the bottom and a current bar along the side of the conical portion of the hull. The prototype of this buoy, unlike the other two, will be made of a glass-reinforced plastic material.

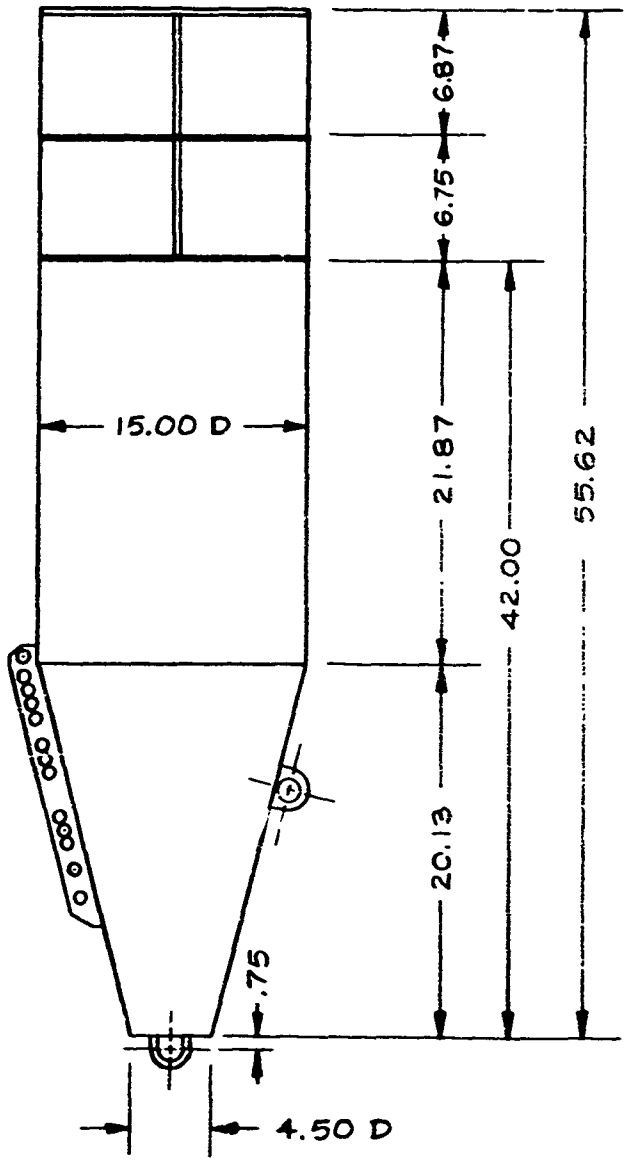

Figure 1. View of ICR Buoy Model

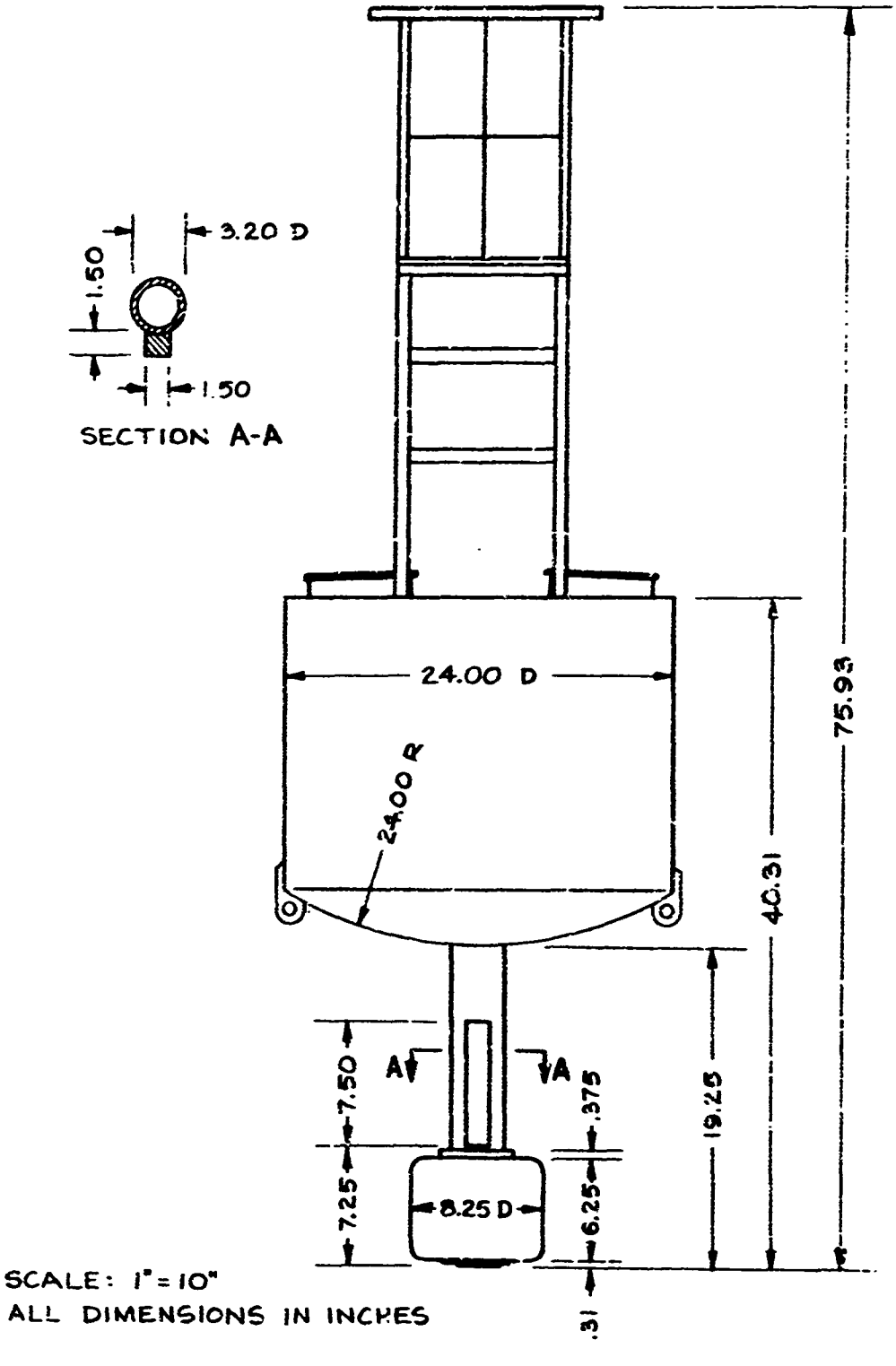

Figure 2. View of 8x26 Buoy Model

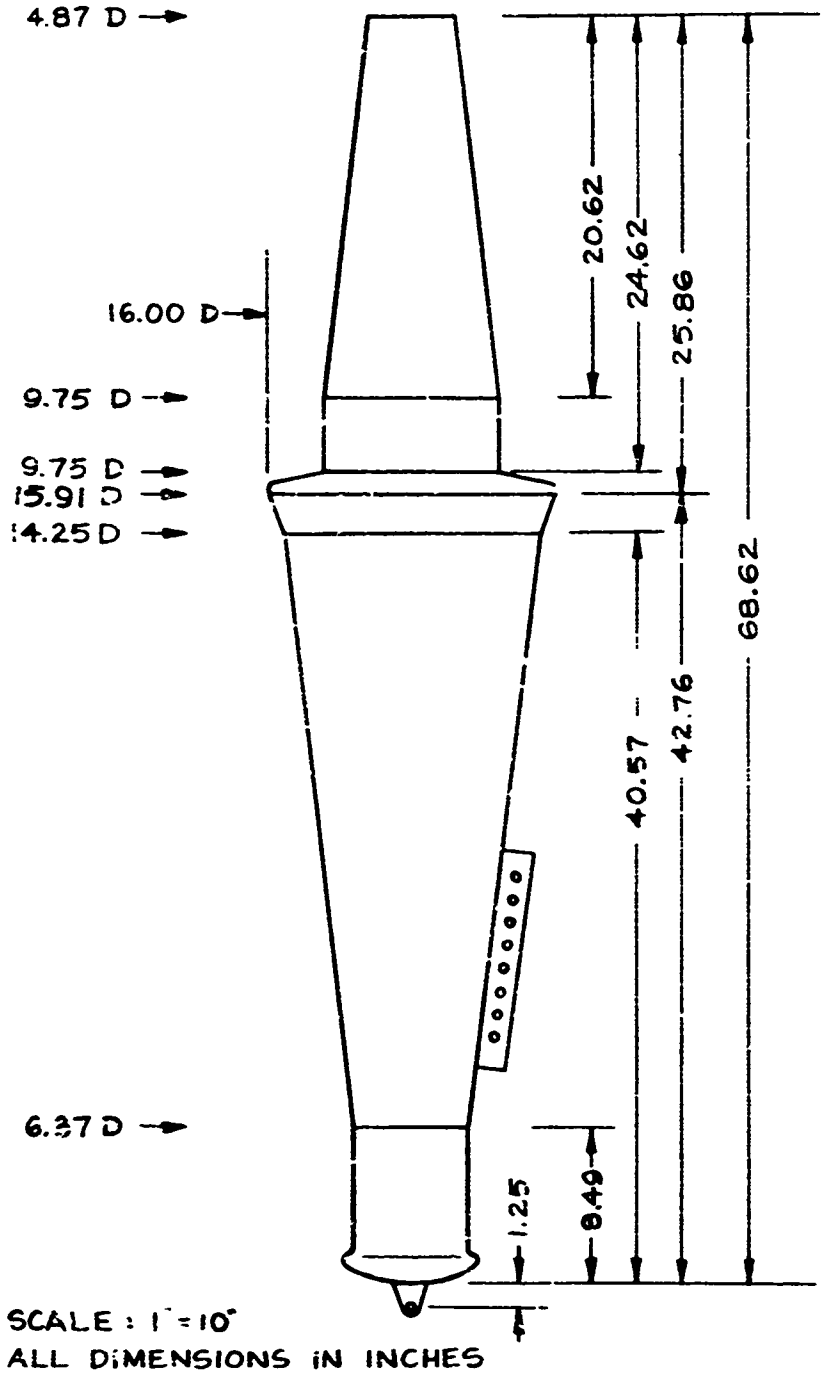

Figure 3. View of CANUN Buoy Model

Section 3

SCALING

It was desired to test 1/4 scale models of the buoys. In order to duplicate the motions of the buoys in a model tank, proper scaling of the buoys' geometric, mechanical and hydrodynamic characteristics is essential. Geometric scaling requires that the model be geometrically similar to the prototype. That is, each dimension of the prototype must correspond to the model: model lengths, in this case are to be $\frac{1}{4}$ of the prototype lengths, angles are to be the same prototype and model. Dynamic scaling requires that: the weight of the model and the total weight of the chain be 1/64 of the prototype buoy and chain, the coordinates of the center of gravity and the gyradius be $\frac{1}{4}$ of the prototype. An analysis of the double pendulum system to determine the gyradius is presented in Appendix A.

Hydrodynamic scaling is, however, less straightforward. Several things must be considered including the effects of the waves and current. Generally, these effects can be decomposed into two parts: free surface effects (such as wave forces, buoyancy, etc.) and viscous effects (such as friction drag on the buoy and flow separation). It is impossible to scale both of these effects properly in a small scale model. We have adopted here the standard technique used in ship model testing in which only the free surface effects are scaled properly. This procedure is called Froude scaling. Here, the wave lengths during the model tests are $\frac{1}{4}$ of the wave lengths of the prototype. This means that, for instance, the ratio of wave length to the maximum buoy diameter is the same for model as for prototype. So a result of Froude scaling, both the model wave period and model current are to be $\frac{1}{2}$ of the corresponding prototype period and current.

Modelling of the viscous effects (called Reynolds scaling) would require larger velocities or smaller viscosity for the model than for the prototype. Since the kinematic viscosity of water is the lowest of the common, useable fluids, and since changes in the velocity would destroy Froude scaling, it was not possible to exactly model these viscous effects. However, it can be shown that the motions produced by the model lead to Reynolds numbers (the measure of the viscous effect) sufficiently large to yield turbulent flow conditions. As a result, the viscous forces are not much dependent on the specific value of Reynolds number and it can be presumed that this discrepancy will not seriously affect the results. It is to be pointed out that motions tests of ship models are also performed without Reynolds scaling and their predictions are satisfactory.

Other hydrodynamic effects such as surface tension, cavitation, roughness, etc. were not explicitly scaled but, from past experience, it can be presumed that these are negligible effects.

The three buoys were Froude-scaled and adjustments were made to the models to account for the testing in fresh rather than salt water. The measured characteristics of the models are given in the following table.

	ICR	8x26	CANUN	CANUN II	CANUN IIa
Weight (lbs.)	83.6	187.0	64.2	69.2	70.0
Center of gravity	17.4*	23.3*	18.2 *	17.1 *	16.9 *
Gyradius (in.)	17.5	19.1	17.1	16.0	15.7
Chain weight per foot	0.70	0.82	0.70	0.30	0.30
Vertical position of moor point (in.)				15.1 *	12.1 *
Horizontal position of moor point (in.)				4.5 ¤	4.1 ¤

* measured from flat bottom of buoy

* measured from bottom dome of buoy

¤ measured from buoy centerline

Measured Physical Characteristics of the Buoys

Section 4

TEST FACILITIES AND INSTRUMENTATION

The tests were performed at Lockheed Missiles & Space Company, Sunnyvale, California. Testing was begun on October 28, 1968 and continued through November 20, 1968. The following is a brief description of the tests, facilities, and instrumentation used:

4.1 LUMF

The primary facility for the testing of the models was the Lockheed Underwater Missile Facility (LUMF). This facility is a wave channel and a test basin equipped with a towing carriage. The speed capability of the carriage is 1.5 to 42 feet per second. The facility is enclosed in a pressure shell and provided with vacuum pumps to permit testing at reduced pressures. Since cavitation is not important for the buoy tests, this feature was not used. The instruments mounted on the tow carriage are connected directly to the data recorders by means of a trailing wire attached to the carriage. No slip-rings are used in this test arrangement. The facility is described in greater detail in Appendix B.

4.2 INSTRUMENTATION

There were four basic pieces of instrumentation used for the buoy tests. There are:

4.2.1 Displacement Probe.

The purpose of this instrument is to measure the position of some point on the buoy at every instant. The probe was designed to give

three signals, each proportional to the three coordinates of the position of the attachment point of the probe to the model. A schematic view of the probe is shown in Figure 4. As seen in this figure, a long arm is attached to the model by means of a ball joint. The upper part of the arm is a $\frac{1}{2}$" square aluminum section; the lower part of the arm is a $\frac{1}{4}$" diameter aluminum rod. The arm is designed so that only the rod section is immersed in the water. A rack is attached to the arm, and a gear mounted to a linear potentiometer is enmeshed with the rack. A set of teflon bearings is mounted in a 1" square steel tube which supports the arm. The steel tube is mounted on ball bearings both in the horizontal plane and vertical plane. The two corresponding axles are connected to precision sine-cosine potentiometers. The voltages across the linear potentiometer are adjusted so the wiper voltage was proportional to the length of the arm. A value of 1 volt per foot was adopted as a standard. The wiper voltage was put through an operational amplifier which followed the voltage and provided a low output impedance. Another operational amplifier was used to create low impedance voltage equal to and opposite in sign to this voltage. These two low impedance signals were placed across the horizontal axis sine-cosine potentiometers to produce two signals. One corresponds to the height (y component) and the other to the radial distance (x' component) of the probe end from the horizontal axis. The voltage of the x' component was put through two operational amplifiers to produce low impedance positive and negative signals. These signals were placed across the vertical axis sine-cosine potentiometer to produce signals proportional to the distance down the tank (x component) and across the tank (z component) from the vertical axis. Three operational amplifiers were used to reduce the impedance of these signals and three more operational amplifiers were used to amplify the signals by ten (for use in obtaining accurate measurements of small motions). All of these signals were recorded on the CEC strip recorder used for these experiments.

4.2.2 Gyro

A Guidance Technology Inc., model 69AA vertical gyro was mounted inside each of the models in order to measure the pitch and roll motions of the buoys. This gyro has a linear potentiometer mounted to the roll and pitch gimbals. A voltage was applied across the potentiometer so that a zero voltage of the wiper corresponded to zero pitch or roll angle. These two signals were also reduced in impedance by use of operational amplifiers and recorded.

4.2.3 Load Cell

A standard 100 lb., 4-arm strain-guage bridge load cell was used for the tests. The cell was fully potted and mounted to the end of the mooring chain. The load cell measured the horizontal component of the chain tension and its instantaneous value recorded.

4.2.4 Wave Gauge

For some of the tests, a capacitance type wave gauge was used to measure the wave height.

4.3 TEST SETUP

Figure 5 shows the setup of the tests. A platform 12' below the water surface was constructed (corresponding to a full scale water depth of 48 feet). The floor of the platform was a smooth plywood. The load cell was attached to various locations on the platform floor so that the buoy position remained within the limits of the displacement probe. The displacement probe was attached to a large "I" beam which, in turn, was bolted to the carriage. The gyro was mounted inside the model at its center of gravity. Tethers were attached to the model to prevent

the buoy from exceeding the maximum excursion of the arm and for pulling the buoy during return of the carriage.

Figure 6 shows the test arrangement for the 1CR buoy and Figure 7 that for the 8x26 buoy. Figure 8 shows details of the CANUN test setup and a view of the counterweight used.

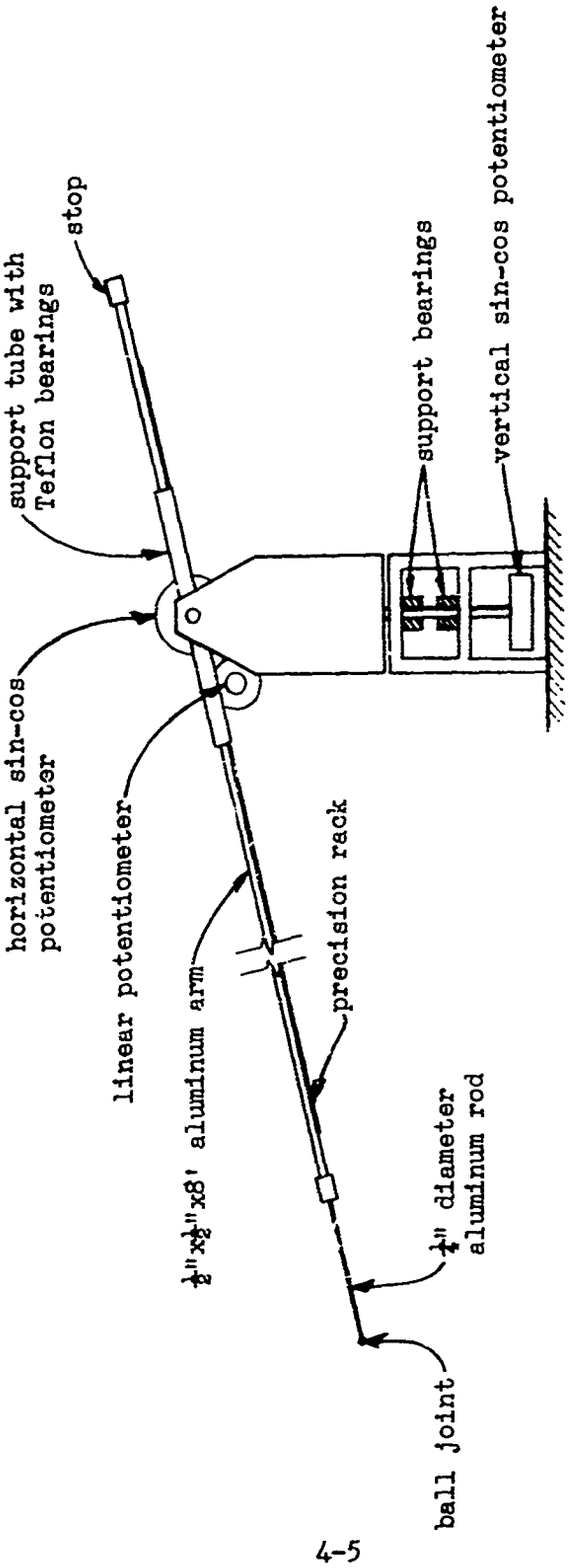

Figure 4. Schematic of Displacement Gauge

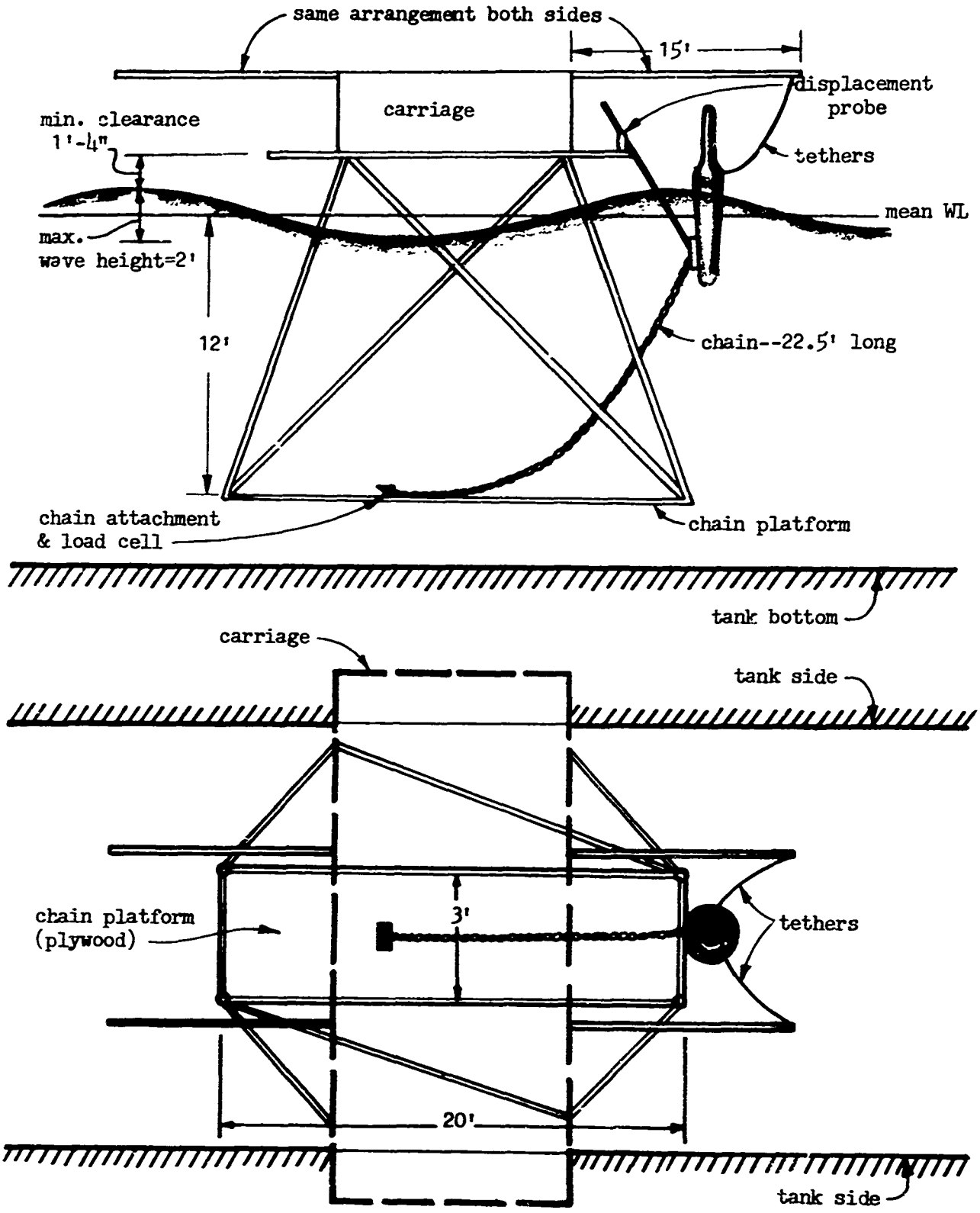

Figure 5. Setup For Buoy Tests

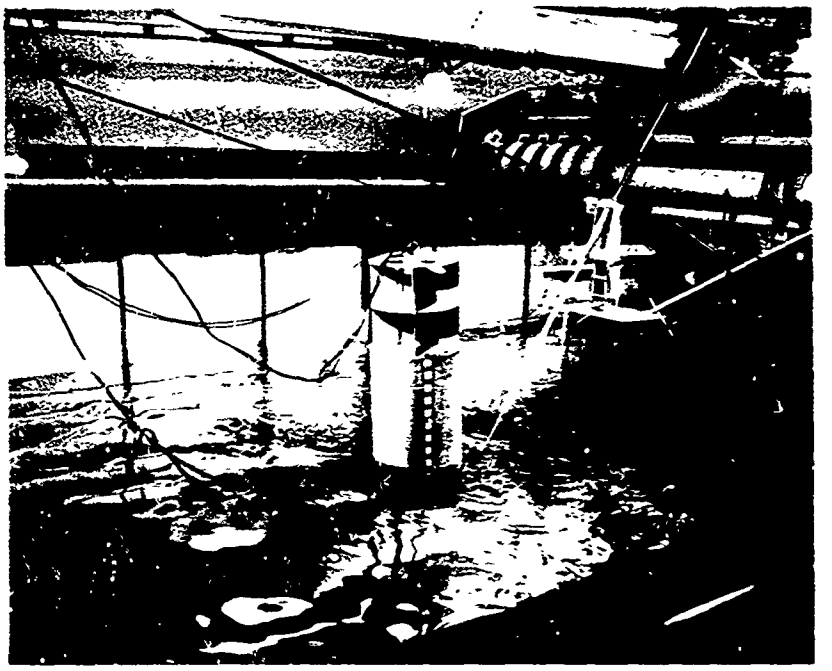

Figure 6. 1CR Buoy Test Setup

Figure 7. 8x26 Buoy Test in Waves

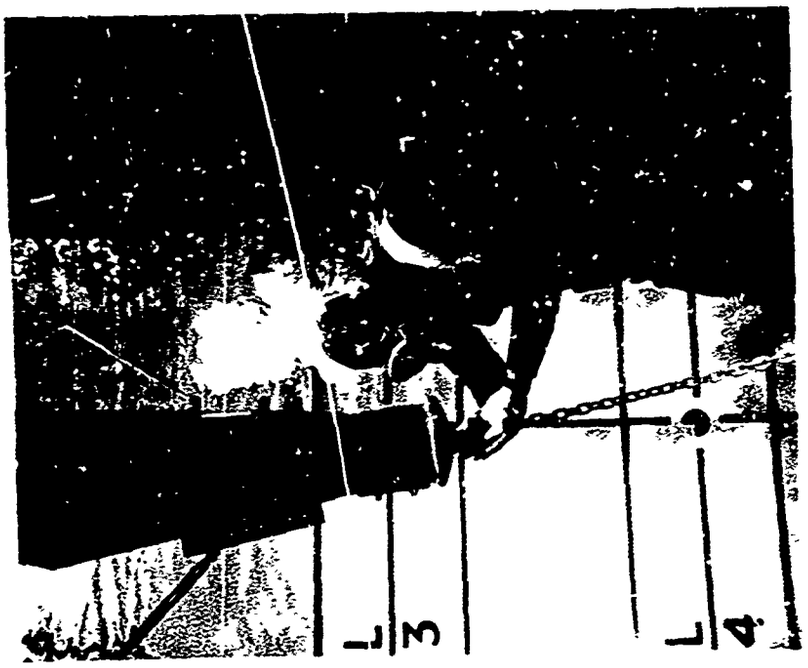

Detail of CANUN II

CANUN Buoy Test in Waves

Figure 8.

Section 5

TEST PROGRAM AND PROCEDURE

5.1 PROGRAM

The test program consisted of two basic parts: tests in waves and tests without waves. A standard series of thirty tests in waves included tests in waves of six different periods (4, 5. 6, 7, 8, 9.2 seconds, full scale) and at five current speeds (-3, -2, 0, +2, +3 knots, full scale). The minus sign in front of the speed indicates a current in the same direction as the wave celerity (following current). The wave height was chosen to correspond to 4 feet, full scale. In addition to the series of tests at this wave height, additional tests at wave heights corresponding to 2 feet and 6 feet full scale were conducted at speeds corresponding to 0, ±3 knots and at a wave period corresponding to 5 seconds. This standard set of tests was performed on the ICR, 8x26 and three versions of the CANUN buoy (the last version of the CANUN buoy was tested only in zero speed and contrary currents).

The tests without waves were conducted on the CANUN buoy only. Here the buoy was towed at various speeds to determine the attitude of the buoy. Additional tests were conducted during which the models were given heave, roll and pitch displacements and the motions subsequent to release recorded. These tests were used to determine the natural frequency and damping decrement of each buoy.

5.2 TEST PROCEDURE

Before the start of any test, the test engineer confirmed that pre-selected settings of the carriage speed control, wave height and wave period were

achieved. When these conditions were met, the wave maker (if used) was turned on and a countdown was initiated where the waves approached the carriage. The countdown procedure included an automatic span check of the load cell. The paper in the strip recorder was started moving at the initiation of the count-down and not stopped until the carriage was stopped or the test ended. After each test, the record was analyzed to assure that the proper carriage speed was achieved.

The instrumentation was checked and calibrated before the tests were undertaken. Subsequently, periodic checks of the calibration were made and corrections, when necessary, were noted. Use was made of these calibrations during the data reduction. Here, the mean values and amplitudes of heave, pitch, roll, sway and surge were determined by scaling the strip chart records. The coordinates for heave and surge were corrected for the distance of the displacement probe end to the center of gravity.

Section 6

TEST RESULTS

The results of the motions of the buoys in scaled 4' waves are shown in Tables 1-5. Each of these tables has two parts. The first part gives the mean values of the pitch, surge and roll motions and the maximum value of the chain tension. The second part gives the amplitudes of the three motions about the means. The data are presented in terms of the full-scale buoys. During many of the tests, the motions of the buoys were not purely sinusoidal, and the values presented in the tables represent averaged means and amplitudes for these tests. The general character of the three motions were similar for all three buoys. The pitch motion displayed a very sharply pronounced resonance. The heave motions displayed only a slight resonance and the surge motion almost none at all. It is to be pointed out that surge motions larger than ½ of the wave height are to be expected in the case of the long period waves. Here, the waves are long enough to be affected by the ocean bottom. The water particle paths are elliptical with the horizontal travel longer than the vertical travel. A brief description of the motions experienced by the three buoys follows.

6.1 THE 1CR BUOY

The 1CR Buoy was tested with the chain attached to the bottom mooring eye for scaled speeds of 0 and $\pm$ 2 knots. For scaled speeds of 3 knots the chain was attached to the 5th hole from the bottom of the current bar. We see from Table 1 that the change in mooring position has a dramatic effect on the average pitch angle assumed by the buoy. The pitch angle varies from approximately 0° at zero speed to about 9° at

a scaled ± 2 knots when the buoy is moored at the bottom eye. This results from the fact that the restraining force acts at the bottom of the buoy and the drag acts at a point near the centroid of the immersed cross-sectional area. The couple produced by these forces causes the large pitch angle under current conditions. When the chain is attached to the current bar the weight of the chain causes a restoring moment. Also, since the attachment point is much closer to the center of drag, less pitch moment is generated. When the buoy was moored at the 5th hole from the bottom on the current bar, the pitch angle was about -2^{o} at 3 knots contrary to the waves and -5^{o} at 3 knots following the waves. The average surge and heave positions were not greatly affected by the change in mooring position. The amplitude of pitch motions indicates a relatively strong resonance for 8 second waves at zero speed. In both following and contrary two knot currents, a resonance occurs for 6 second waves. This peak was predominately a non-linear subharmonic resonance.

Here, waves with one-half of the period of the pitch resonance caused significant motions of the buoy. This seaway caused very large motions every other wave. In other words, there is a strong double period motion. Since the waves themselves do not have any energy at this frequency, it is clearly a second-order effect.

The surge and heave amplitudes were more or less resonance free. Some magnification of the heave amplitude occurred in the case of current following the waves.

During the tests of all of the buoys, particularly the tests of the 1CR in which the chain was attached to the current bar, the buoy tended to wander from side to side in a random, irreproducible fashion. Because of this randomness, it was not possible nor was it significant, to present this sway data in a coherent form. It is believed that the

wander is due to hydrodynamic lift forces created on the buoy due to vortex shedding around this rather unstreamlined form. At these high Reynolds numbers turbulent flow conditions exist, and the shedding is not periodic. This randomness can account for the random wandering. Furthermore, the buoy was arranged with the current bar on the upstream side of the buoy. This bar appeared to dramatically worsen the wander problem. The current bar seemed to make the buoy unstable in yaw in a current. The large yaw motions induced large roll motions as well. The following is a brief description of the process. When the current bar is not quite aligned with the flow, lift forces are generated on it in such a way as to yaw the buoy more. These lift forces, because they are below the center of gravity, also cause roll motions. The yaw angle and roll motion continue to grow until either the chain force or wave force cause it to return and begin again.

In addition to the above mentioned wander problem, the 1CR buoy occasionally demonstrated a heave-roll instability. In general there was very little roll motion except for random rolling directly attributable to the above mentioned wandering. Under certain conditions, a heave-roll instability occurred in which very large, periodic rolling was observed. This motion, sometimes observed in ships also, occurs due to non-linearities in the roll restoring mechanism. The heave motion causes a roll motion which is at one-half the frequency of the heave. The roll motion becomes unstable and continues to grow until some limiting process is encountered. During one test of the 1CR buoy, roll motions as much as $\pm 70^{\circ}$ were observed during one instance of the instability. Because in all instances, roll could be attributed to either non-periodic wandering effects or this non-steady, heave-roll instability, it was not possible to present this roll data in a coherent or meaningful form.

6.2 THE 8x26 BUOY

The motions of the 8x26 buoy were, in general, much better behaved than the 1CR. The test results are displayed in Table 2. The average pitch angles for the range between -3 to 3 knots varied from about 0 degrees to about 5 degrees. This small range is due primarily to the bridal mooring system which allows the chain load to be transmitted directly to a point near the center of lateral effort. It is believed that the large average pitch angle for the case of the 4 second wave at 3 knots was due primarily to the near-surface mass transport velocity induced by the short waves. The mean surge position of the buoy increases in a regular way with the current. It is interesting to note that the mean heave position of the buoy becomes positive for the cases of forward velocity. That is, the buoy rides higher in the water than at zero speed. Apparently this effect is due to planing of the dome-shaped bottom of the buoy. The positive average pitch angles of the buoy in a current provide the proper angle of attack for such planing.

The 8x26 buoy shows a very pronounced pitch resonance in 6 second waves at zero speed. This resonance is also exhibited at slightly longer period waves for contrary currents and slightly shorter period waves for following currents. A slight surge and heave resonance also occurs near the six second period.

6.3 THE CANUN BUOY SERIES

Three different configurations of the CANUN buoy were tested. The first configuration corresponded to the buoy as originally submitted for testing. The second two configurations represented refinements of this design resulting from tests of the first configuration. To distinguish the last two configurations from the first, they will be referred hereafter by the names CANUN II and CANUN IIa.

6.3.1 CANUN

This buoy was moored at the bottom eye for 0 speed and scaled ± 2 knots. For scaled ± 3 knots the buoy was moored at the second hole from the bottom of the current bar. From Table 3, we see that the change in mooring point has a dramatic effect on the average pitch angle. The pitch angle varies from near 0° at 0 speed to about 9° at a scaled ± 2 knots, when moored at the bottom eye. When moored at the second hole from the bottom of the current bar the pitch angle is 16.1° at 0 speed and is about 2° at a scaled 3 knots. Thus, it was determined that no individual mooring location gave satisfactory pitch angles to the buoy over the range of 0 speed to 3 knots. The average heave position was well behaved, decreasing with increasing speed. The average surge position was rather more at 2 knots than the other buoys. The surge position was measured at the center of gravity. Although the chain displacement was comparable to the other buoys, the much larger distance from the moor point to the center of gravity combined with the large average pitch angle contributed to the large values of average surge position. The amplitudes of the pitch, heave and surge motions all appear well behaved. The tests at 3 knots showed a current-bar induced yaw instability similar to the 1CR buoys.

6.3.2 CANUN II

In an effort to improve the variation of the average pitch angle with the current, a single point mooring system was developed. (See Appendix C) This system employs a mooring location on the side of the buoy (for the tests it was mounted opposite to the current bar) and a counterweight mounted to the lower cylindrical portion of the buoy. The counterweight and mooring point were on opposite sides of the buoy and the weight was chosen so that the buoy would also be vertical at 3 knots. The results shown in Table 4 demonstrate that the objective of near-zero pitch angle

was achieved. However, the change from the previous mooring situation to the single point moor, produced excessively large amplitudes of motion. It was apparent that both the pitch and roll damping of this new configuration was very small, and, as a result, pitch-roll coupled motions were observed. In addition, the pitch and roll resonant frequencies were nearly coincident. As a result, the energy of rolling was easily shared with the energy of pitching and vice versa. The large pitching motions experienced at zero speed (as a result of low pitch damping) caused almost equally large roll motions. In addition to the above mentioned pitch-roll motions, some instances of heave-roll instability (described in 5.1 above) were also experienced. It was felt that the attitude performance of the buoy was satisfactory but its motions were not. This led to the following configuration.

6.3.3 CANUN IIa

A pitch damper was added to the bottom of the buoy passing over the mooring eye as shown in figure 9. This damper dramatically improved the pitch and roll characteristics of the buoy. Because this addition also lowered the lateral center of effort (the point at which the drag appears to be acting), the mooring point also had to be lowered. Tests were conducted at zero current and contrary currents only. The average position results are shown in Table 5. Here, we see that these results are comparable to the CANUN II above. The maximum horizontal chain tensions are somewhat larger but this is to be expected in light of the increased drag of the damper. The motion amplitudes, particularly the pitch amplitude is considerably better than the CANUN II.

During these tests, it became apparent that the heave damping caused by the bottom plate of the damper was too great. The diminished heave motions led to several instances where the buoy was far enough out of water to have negative pitch stability. The buoy then "fell over" until

the stability was restored. This was the primary reason for the large motions observed in the long period waves at a scaled 3 knots. Subsequent to the CANUN IIa tests the bottom plate of the damper was significantly cut away, as shown in figure 9. Tests on this buoy performed in conjunction with the shooting documentary did not show this heave-pitch instability.

6.4 TESTS IN VARIOUS WAVE HEIGHTS

Tests were performed in scaled 2', 4' and 6' wave heights for all five buoy configurations. These results are presented in Table 6. In general, it is seen that the motions increase monotonically with wave height. The motions per foot wave height are, in most cases, smaller for the higher wave heights than for the lower wave heights. This result is believed due to non-linear effects, particularly, the quadratic damping terms.

6.5 THE BUOY ATTITUDE

It is important to know the mean value of pitch, surge and heave to be expected under conditions of an ordinary seaway. For this purpose, the values shown for these positions in tables were averaged over the wave periods tested. The mean pitch results are shown in figure 10, the mean surge results in figure 11 and the mean heave results in figure 12. In addition, tests in current and no waves were made for the CANUN II and CANUN IIa buoys. The results for the mean pitch and heave are shown in figure 13. Note that the pitch variation agrees quite well with the theoretical pitch moment shown in Appendix C.

Average Surge Position, Feet						
Current Knots	Wave Period, Seconds					
	4.0	5.0	6.0	7.0	8.0	9.2
3	28.5	28.6	28.8	28.8	28.0	28.5
2	22.7	21.2	21.2	22.2	22.3	22.2
0	-0.1	0.2	-0.4	0.1	-0.1	0.5
-2	20.1	17.1	18.5	19.8	21.0	22.6
-3	27.2	26.6	27.6	27.5	27.5	27.7

Average Heave Position, Feet						
Current Knots	Wave Period, Seconds					
	4.0	5.0	6.0	7.0	8.0	9.2
3	-2.3	-1.8	-1.6	-2.0	-1.8	-1.6
2	-1.6	-1.0	-1.3	-1.3	-1.2	-1.3
0	0.0	0.0	0.1	0.0	0.0	0.0
-2	-1.3	-1.3	-1.6	-1.1	-1.2	-1.1
-3	-2.1	-1.8	-1.9	-2.1	-1.5	-1.7

Average Pitch Angle, Degrees						
Current Knots	Wave Period, Seconds					
	4.0	5.0	6.0	7.0	8.0	9.2
3	4.0	-3.3	-2.1	-1.4	-4.1	-3.7
2	12.1	8.3	6.9	9.9	9.8	7.3
0	0.0	1.2	0.0	0.7	0.0	1.0
-2	5.9	9.5	10.7	7.6	9.6	9.3
-3	-4.2	-4.0	-4.0	-3.8	-6.1	-4.2

Maximum Horizontal Chain Tension, Pounds						
Current Knots	Wave Period, Seconds					
	4.0	5.0	6.0	7.0	8.0	9.2
3	2000	1510	1680	1690	1010	960
2	490	420	390	420	440	480
0	0	0	0	0	0	0
-2*	400	300	340	420	400	470
-3*	1360	1110	1470	1810	1530	1200

0 and ±2 knots current - buoy moored on bottom eye

±3 knots - buoy moored on 5th hole from bottom of current bar

* load cell inoperative, horizontal chain tension computed

Table 1. Average Surge Positions, Heave Positions, Pitch Angles and Maximum Horizontal Chain Tensions for 1CR Buoy.

Pitch Amplitude, Degrees						
Current Knots	Wave Period, Seconds					
	4.0	5.0	6.0	7.0	8.0	9.2
3	8.6	11.6	12.5	8.4*	5.6*	5.7*
2	6.2	8.0	12.8	8.6	7.2	7.2
0	1.3	2.3	4.5	7.4	10.5	3.2
-2	8.1	9.2	10.0	6.4	4.0	1.9
-3	13.6	9.0	8.0	9.5	6.0	3.2
Heave Amplitude, Feet						
Current Knots	Wave Period, Seconds					
	4.0	5.0	6.0	7.0	8.0	9.2
3	1.7	1.8	1.9	1.8	1.9	1.8
2	2.2	2.0	1.8	2.4	2.2	2.2
0	2.1	1.8	1.9	1.8	2.5	2.0
-2	1.9	2.0	2.2	2.0	2.0	1.8
-3	1.7	1.8	2.3	1.8	1.9	2.0
Surge Amplitude, Feet						
Current Knots	Wave Period, Seconds					
	4.0	5.0	6.0	7.0	8.0	9.2
3	1.0	1.3	1.4	1.5	1.4	1.7
2	1.2	1.3	1.7	2.0	2.3	2.8
0	2.2	1.9	1.7	2.9	2.3	3.0
-2	2.1	2.6	2.9	2.7	2.8	3.2
-3	2.0	2.2	2.4	2.2	2.8	2.0

0 and ±2 knots current - buoy moored on bottom eye

±3 knots current - buoy moored on 5th hole from bottom of current bar

* heave-roll instability present

Table 1 (Cont'd). The Pitch, Heave and Surge Amplitudes for the ICR Buoy

Average Surge Position, Feet						
Current Knots	Wave Period, Seconds					
	4.0	5.0	6.0	7.0	8.0	9.2
3	31.9	29.8	30.1	30.0	29.5	29.3
2	29.0	23.0	22.9	22.9	22.2	22.3
0	2.8	1.2	0.0	-0.1	0.0	-0.1
-2	11.8	20.6	20.5	20.2	20.6	20.4
-3	27.5	29.0	29.5	29.2	29.0	29.6

Average Heave Position, Feet						
Current Knots	Wave Period, Seconds					
	4.0	5.0	6.0	7.0	8.0	9.2
3	0.3	0.4	0.0	0.3	0.5	0.5
2	0.5	0.5	0.1	0.4	0.4	0.4
0	0.0	0.0	0.2	-0.2	-0.2	0.0
-2	1.0	0.6	0.8	0.8	0.9	0.9
-3	0.9	0.7	0.9	0.8	0.7	0.5

Average Pitch Angle, Degrees						
Current Knots	Wave Period, Seconds					
	4.0	5.0	6.0	7.0	8.0	9.2
3	10.1	4.0	4.9	4.1	3.9	5.7
2	5.2	2.2	2.2	2.8	3.2	3.2
0	-0.6	-0.7	-0.2	-0.2	-0.1	0.1
-2	-1.4	-0.5	0.1	2.4	2.6	1.9
-3	2.3	2.6	5.5	4.2	5.4	3.9

Maximum Horizontal Chain Tension, Pounds						
Current Knots	Wave Period, Seconds					
	4.0	5.0	6.0	7.0	8.0	9.2
3*	4010	2190	2340	2600	1730	1910
2*	1350	590	620	630	570	630
0*	0	0	0	0	0	0
-2*	320	470	480	600	490	500
-3*	1260	1900	2500	2830	2220	1970

* load cell inoperative, horizontal chain tension computed

Table 2. Average Surge Positions, Heave Positions, Pitch Angles, and Maximum Horizontal Chain Tensions for 8x26 Buoy.

Pitch Amplitude, Degrees						
Current Knots	Wave Period, Seconds					
	4.0	5.0	6.0	7.0	8.0	9.2
3	5.4	9.1	14.8	13.8	6.5	4.5
2	6.0	8.3	13.6	9.6	4.7	4.5
0	8.0	17.1	21.0	6.1	3.3	2.2
-2	28.0	20.8	10.1	6.3	3.4	2.5
-3	21.6	13.5	8.0	4.4	2.4	2.8
Heave Amplitude, Feet						
Current Knots	Wave Period, Seconds					
	4.0	5.0	6.0	7.0	8.0	9.2
3	2.2	2.6	3.0	3.3	2.3	2.2
2	2.3	2.3	2.9	2.8	2.2	2.2
0	2.5	3.0	3.3	2.4	2.0	2.0
-2	2.4	2.2	2.0	1.8	2.0	1.9
-3	2.0	2.2	2.4	2.0	1.9	1.8
Surge Amplitude, Feet						
Current Knots	Wave Period, Seconds					
	4.0	5.0	6.0	7.0	8.0	9.2
3	0.8	1.0	1.6	1.7	1.9	2.4
2	1.5	1.7	1.9	2.1	2.4	3.0
0	1.9	2.8	3.0	2.3	2.2	2.8
-2	2.0	2.5	2.8	3.1	2.8	3.3
-3	2.8	2.7	3.0	3.3	3.2	3.4

Table 2 (Cont'd). The pitch, heave and Surge Amplitudes for the 8x26 Buoy

Average Surge Position, Feet						
Current Knots	Wave Period, Seconds					
	4.0	5.0	6.0	7.0	8.0	9.2
3	*	30.8	29.9	30.0	30.4	30.6
2	28.6	29.1	27.9	28.3	27.6	26.6
0	1.4	0.7	0.0	-0.5	-0.6	0.5
-2	25.3	26.5	26.8	27.7	25.9	24.2
-3	28.0	27.5	27.8	27.9	29.2	28.3

Average Heave Position, Feet						
Current Knots	Wave Period, Seconds					
	4.0	5.0	6.0	7.0	8.0	9.2
3	*	-2.7	-2.9	-2.9	-2.7	-2.8
2	-1.0	-1.5	-1.5	-1.7	-1.2	-0.9
0	-0.3	0.0	-0.2	0.0	0.0	-0.2
-2	-0.6	-0.8	-0.6	-0.6	-0.8	-0.6
-3	-2.1	-2.1	-2.0	-2.2	-2.4	-2.1

Average Pitch Angle, Degrees						
Current Knots	Wave Period, Seconds					
	4.0	5.0	6.0	7.0	8.0	9.2
3	*	2.3	2.0	2.3	3.9	4.7
2	13.4	10.0	9.9	8.9	8.9	11.0
0	0.5	1.1	-0.9	-1.5	-1.6	-1.9
-2	8.4	10.2	8.1	7.2	7.7	6.8
-3	4.1	1.6	-0.9	0.0	3.8	-0.2

Maximum Horizontal Chain Tension, Pounds						
Current Knots	Wave Period, Seconds					
	4.0	5.0	6.0	7.0	8.0	9.2
3	*	1200	1030	1200	1030	1150
2	690	590	540	600	540	240
0	0	0	0	0	0	0
-2	450	460	510	490	390	330
-3	830	840	790	910	1030	890

0 and ±2 knots current - buoy moored on bottom eye.

±3 knots current - buoy moored on 5th hole from bottom of current bar.

* test record faded, cannot be read

Table 3. Average Surge Positions, Heave Positions, Pitch Angles and Maximum Horizontal Chain Tensions for CANUN Buoy.

Pitch Amplitude, Degrees						
Current Knots	Wave Period, Seconds					
	4.0	5.0	6.0	7.0	8.0	9.2
3	*	11.5	9.9	9.0	6.0	6.5□
2	11.1	10.4	7.6	6.6	4.2	8.7□
0	10.8	15.0	18.7	5.6	3.4	2.2
-2	10.5	8.1	6.1	3.8	3.0	3.0
-3	8.1	6.3	4.7	3.8	3.8	3.0

Heave Amplitude, Feet						
Current Knots	Wave Period, Seconds					
	4.0	5.0	6.0	7.0	8.0	9.2
3	*	2.2	2.4	1.7	1.8	1.6
2	2.4	2.5	2.1	1.9	2.0	1.8
0	2.5	2.5	2.5	2.4	2.0	2.0
-2	1.6	1.6	2.3	2.0	2.0	1.9
-3	1.6	1.9	2.0	2.0	2.0	1.9

Surge Amplitude, Feet						
Current Knots	Wave Period, Seconds					
	4.0	5.0	6.0	7.0	8.0	9.2
3	*	0.9	1.4	1.7	1.8	2.2
2	1.6	2.4	2.6	2.0	1.7	2.4
0	1.8	2.0	2.0	2.0	1.9	2.6
-2	2.4	3.2	2.5	3.0	3.4	3.3
-3	2.6	2.6	2.9	3.2	2.6	2.8

0 and ±2 knots current - buoy moored on bottom eye

±3 knots current - buoy moored on 2nd hole from bottom of current bar

* test record faded, cannot be read

□ large roll motions due to wandering

Table 3 (Cont'd). The Pitch, Heave and Surge Amplitudes for the CANUN Buoy

Average Surge Position, Feet						
Current Knots	Wave Period, Seconds					
	4.0	5.0	6.0	7.0	8.0	9.2
3	30.5	30.3	30.6	30.3	30.5	29.5
2	*	20.3	19.4	21.1	21.5	22.3
0	-0.1	0.1	0.2	0.1	-0.1	-0.2
-2	20.9	19.5	21.5	21.7	22.2	20.9
-3	30.0	29.1	29.6	29.8	29.0	29.6

Average Heave Position, Feet						
Current Knots	Wave Period, Seconds					
	4.0	5.0	6.0	7.0	8.0	9.2
3	-1.8	-2.1	-2.0	-1.9	-1.7	-1.7
2	*	-0.7	-1.0	-0.8	-0.6	-0.9
0	0.3	0.0	0.3	0.1	-0.2	-0.1
-2	-0.5	-0.4	-1.0	-0.6	-0.8	-0.5
-3	-1.5	-1.5	-1.4	-1.2	-1.8	-1.5

Average Pitch Angle, Degrees						
Current Knots	Wave Period, Seconds					
	4.0	5.0	6.0	7.0	8.0	9.2
3	5.6	2.6	1.2	1.0	-0.7	-2.1
2	*	0.6	-3.1	-3.2	-3.0	-3.4
0	-1.7	-2.1	-2.4	-2.7	-2.9	-1.6
-2	-3.5	-3.2	-1.7	-3.0	-2.6	-4.5
-3	-0.3	-0.4	1.1	-1.1	-1.6	-3.1

Maximum Horizontal Chain Tension, Pounds						
Current Knots	Wave Period, Seconds					
	4.0	5.0	6.0	7.0	8.0	9.2
3	1790	1270	1050	1230	1230	1130
2	*	300	370	450	350	270
0	0	0	0	0	0	0
-2	220	190	240	250	280	200
-3	930	790	1180	950	1110	770

* motions too severe to test

Table 4. Average Surge Positions, Heave Positions, Pitch Angles, and Maximum Horizontal Chain Tensions for CANUN II.

Pitch Amplitude, Degrees						
Current Knots	Wave Period, Seconds					
	4.0	5.0	6.0	7.0	8.0	9.2
3	10.3	15.8	7.9	7.5	7.1	5.5
2	*	20.4	15.8	6.4	2.5	2.8
0	12.0	26.2	18.8	14.0	10.0	4.5
-2	26.6	20.0	11.1	9.5	4.6	4.6
-3	11.6	7.6	6.1	4.6	3.8	3.7
Heave Amplitude, Feet						
Current Knots	Wave Period, Seconds					
	4.0	5.0	6.0	7.0	8.0	9.2
3	1.6	1.8	2.2	1.8	1.5	1.5
2	*	2.5	2.7	2.2	1.7	1.8
0	2.9	3.0	3.3	2.1	2.1	1.8
-2	1.8	2.0	2.2	1.9	1.9	1.8
-3	2.0	2.1	2.2	2.2	2.0	2.0
Surge Amplitude, Feet						
Current Knots	Wave Period, Seconds					
	4.0	5.0	6.0	7.0	8.0	9.2
3	1.0	1.0	0.9	1.2	1.2	1.6
2	*	1.8	1.2	1.2	1.5	2.4
0	1.5	1.8	2.3	1.6	2.1	1.8
-2	2.0	2.4	3.0	3.2	2.9	3.3
-3	2.0	2.5	2.9	3.0	3.0	2.6

* motions too severe to test

note: all tests exhibited roll-pitch coupled motions

Table 4 (Cont'd). The Pitch, Heave and Surge Amplitudes for the CANUN II Buoy

Average Surge Position, Feet						
Current Knots	Wave Period, Seconds					
	4.0	5.0	6.0	7.0	8.0	9.2
3	30.7	31.3	30.9	31.3	30.8	31.0
2	23.2	22.8	22.3	22.9	22.1	22.7
0	0.2	0.4	-0.4	0.0	-0.2	0.0
-2	not tested					
-3						

Average Heave Position, Feet						
Current Knots	Wave Period, Seconds					
	4.0	5.0	6.0	7.0	8.0	9.2
3	-1.8	-1.9	-1.9	-2.0	-2.0	-1.8
2	-1.2	-1.4	-1.4	-1.5	-1.1	-1.2
0	-0.1	0.2	0.2	-0.1	0.2	0.0
-2	not tested					
-3						

Average Pitch Angle, Degrees						
Current Knots	Wave Period, Seconds					
	4.0	5.0	6.0	7.0	8.0	9.2
3	1.2	-0.5	-0.7	2.8	1.2	1.4
2	0.4	-2.1	-3.8	-2.5	-3.6	-3.0
0	0.7	-0.1	-0.3	-1.9	-1.2	-1.6
-2	not tested					
-3						

Maximum Horizontal Chain Tension, Pounds						
Current Knots	Wave Period, Seconds					
	4.0	5.0	6.0	7.0	8.0	9.2
3	2060	1700	1730	1940	1690	1920
2	880	730	810	770	560	670
0	0	0	0	0	0	0
-2	not tested					
-3						

Table 5. Average Surge Positions, Heave Positions, Pitch Angles and Maximum Horizontal Chain Tensions for CANUN IIa Buoy.

Pitch Amplitude, Degrees						
Current Knots	Wave Period, Seconds					
	4.0	5.0	6.0	7.0	8.0	9.2
3	9.6	10.2	11.4	8.2	7.6*	6.7*
2	9.4	11.9	8.9	7.2	5.0	3.7
0	7.6	14.1	18.1	15.6	6.6	4.8
-2	not tested					
-3						

Heave Amplitude, Feet						
Current Knots	Wave Period, Seconds					
	4.0	5.0	6.0	7.0	8.0	9.2
3	1.3	1.6	1.5	1.2	1.3	1.4
2	2.3	2.1	2.0	2.0	2.1	1.8
0	2.5	2.5	2.5	2.8	2.3	1.9
-2	not tested					
-3						

Surge Amplitude, Feet						
Current Knots	Wave Period, Seconds					
	4.0	5.0	6.0	7.0	8.0	9.2
3	0.8	0.8	1.1	1.3	1.3	1.3
2	1.2	1.5	1.6	2.1	1.8	2.2
0	1.9	2.0	2.7	2.3	2.1	2.3
-2	not tested					
-3						

* motions not simusoidal, excessive heave damping effects

Table 5 (Cont'd). The Pitch, Heave and Surge Amplitudes for the CANUN IIa Buoy

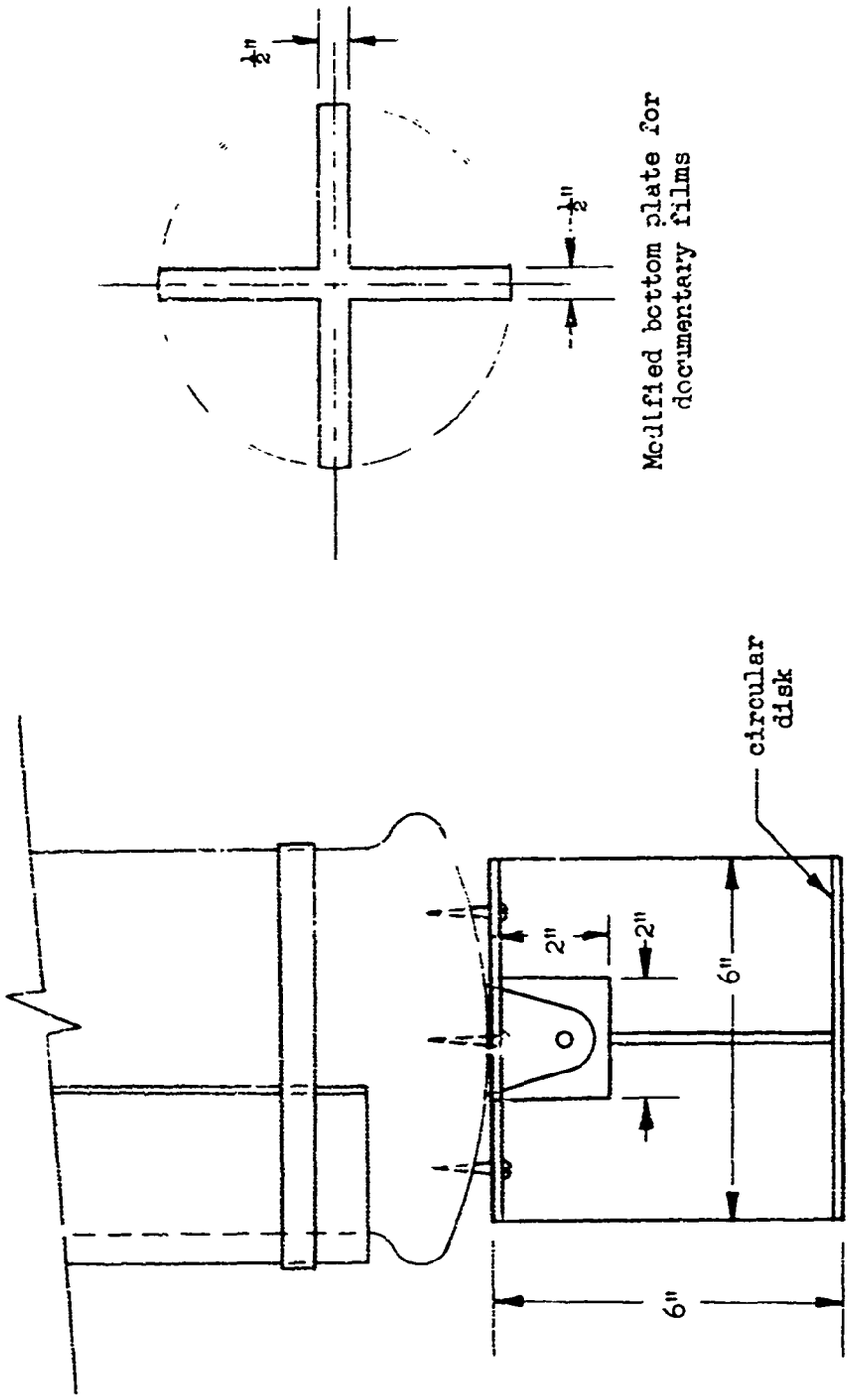

Figure 9. CANUN IIa Configurations

8x26
Buoy

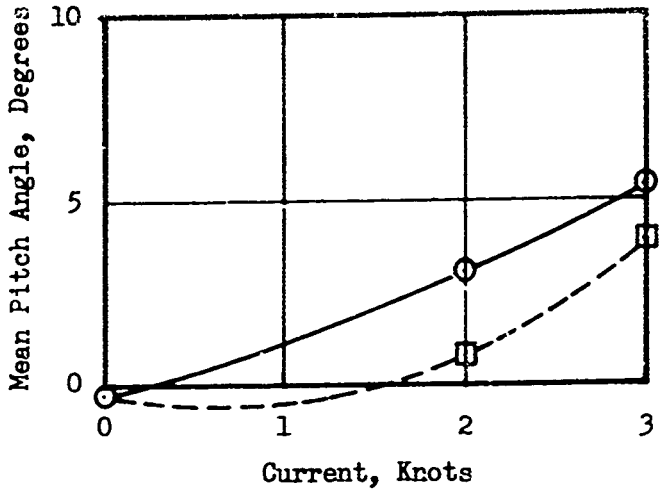

1CR
Buoy

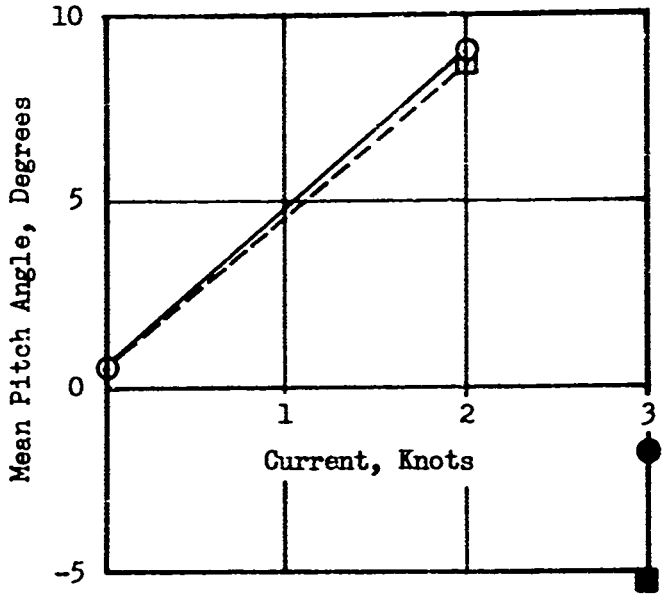

○ Current and wave celerity same direction

□ Current and wave celerity opposite directions

Solid symbol indicates change in mooring point

Figure 10. Variation of Mean Pitch Angle with Current

CANUN Buoy

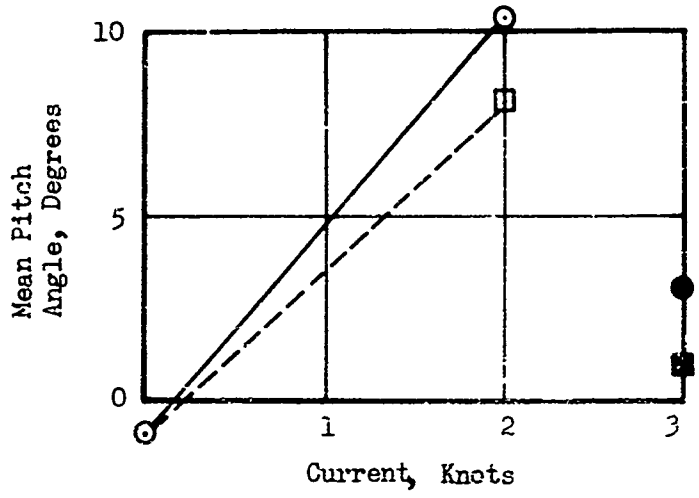

CANUN II Buoy

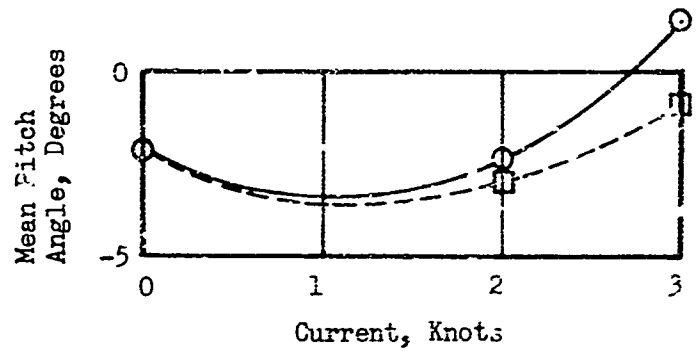

CANUN IIa Buoy

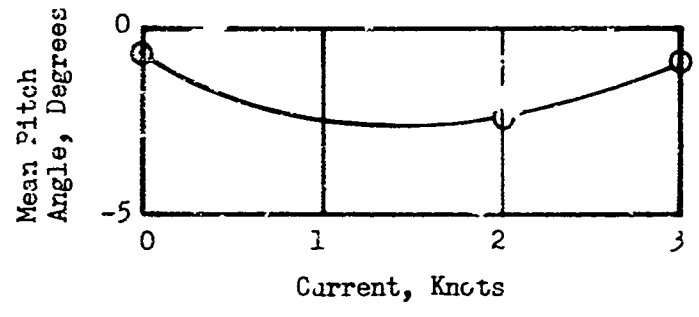

○ Current and wave celerity same direction

□ Current and wave celerity opposite directions

Solid symbol indicates change in mooring point

Figure 10 (cont'd). Variation of Mean Pitch Angle with Current

8x26
Buoy

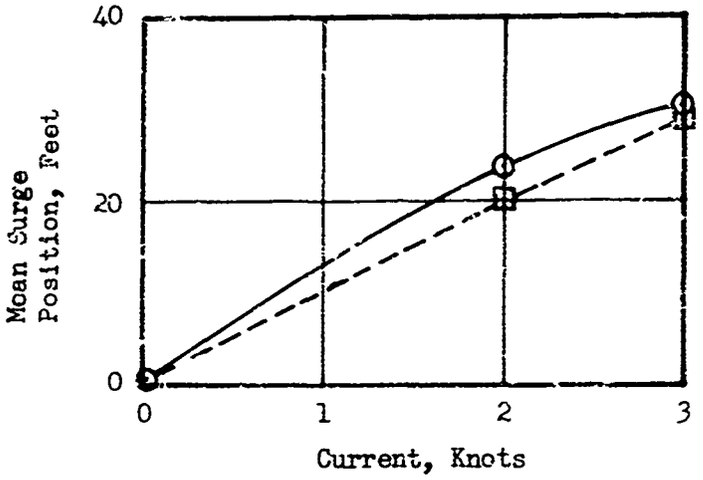

1CR
Buoy

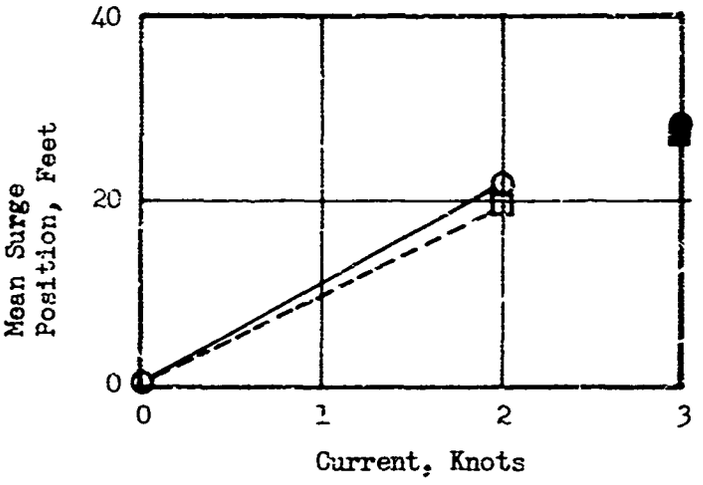

○ Current and wave celerity same direction

□ Current and wave celerity opposite directions

Solid symbol indicates change in mooring point

Figure 11. Variation of Mean Surge Position with Current

CANUN Buoy

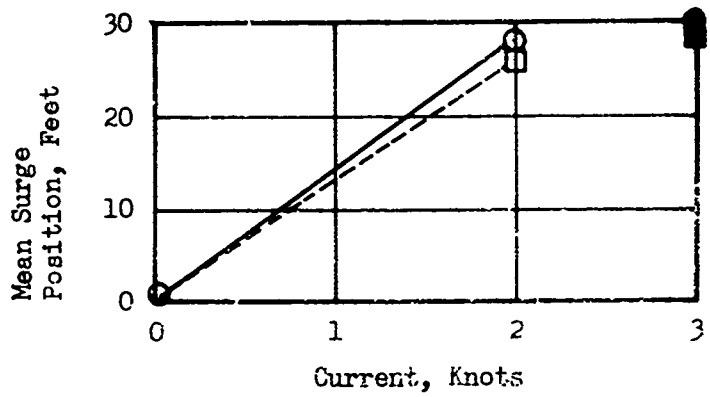

CANUN II Buoy

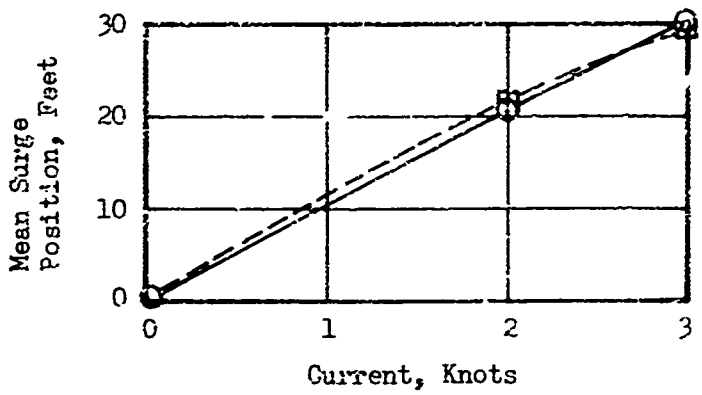

CANUN IIa Buoy

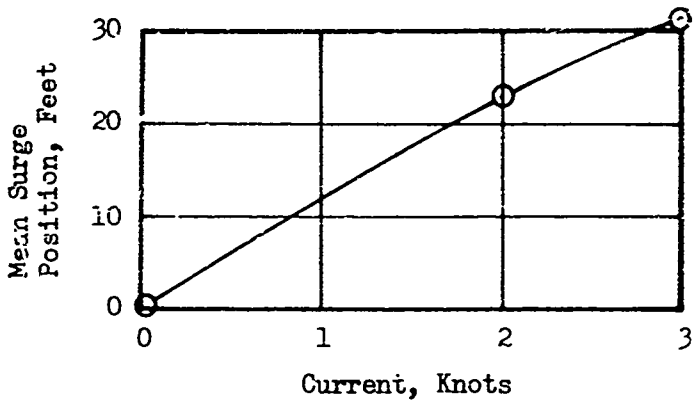

○ Current and wave celerity same direction

□ Current and wave celerity opposite directions

Solid symbols indicates change in mooring points

Figure 11 (Cont'd). Variation of Mean Surge Position with Current

8x26 Buoy

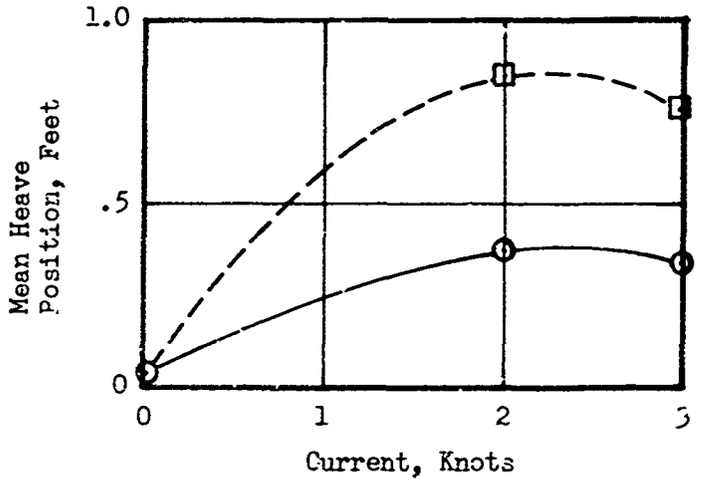

1CR Buoy

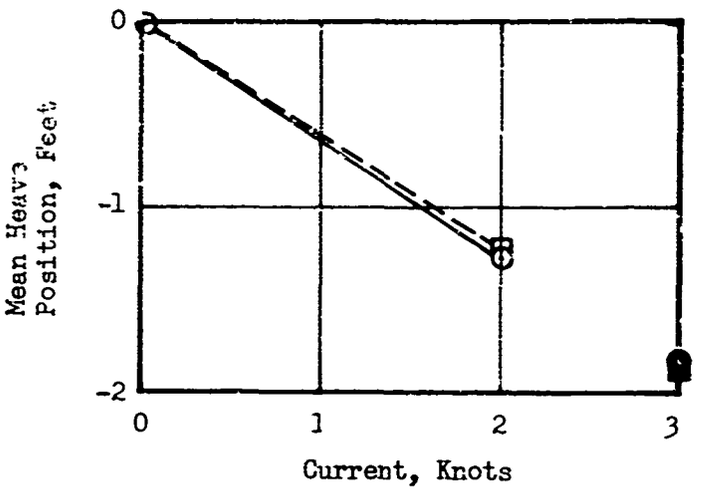

○ Current and wave celerity same direction

□ Current and wave celerity opposite directions

Solid symbol indicates change in mooring point

Figure 12. Variation of Mean Heave Position with Current

CANUN Buoy

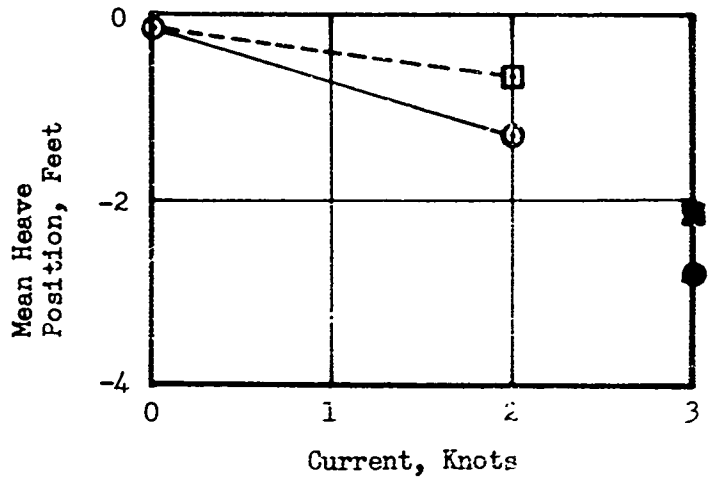

CANUN II Buoy

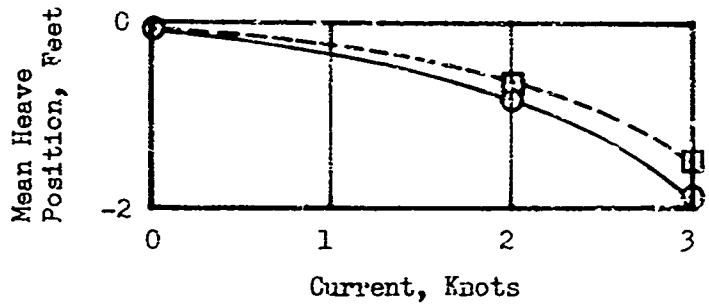

CANUN IIa Buoy

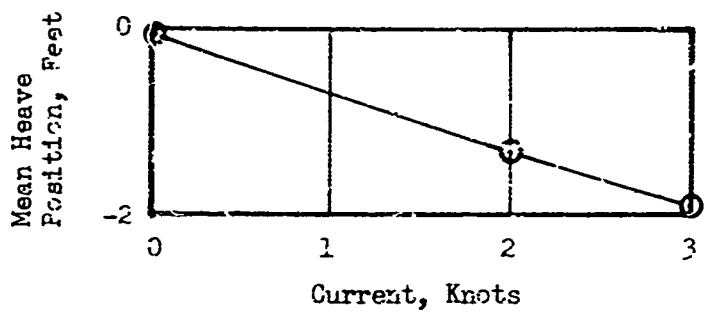

○ Current and wave celerity same direction

□ Current and wave celerity opposite directions

Solid symbol indicates change in mooring point

Figure 2.2 (Cont'd). Variation of Mean Heave Position with Current

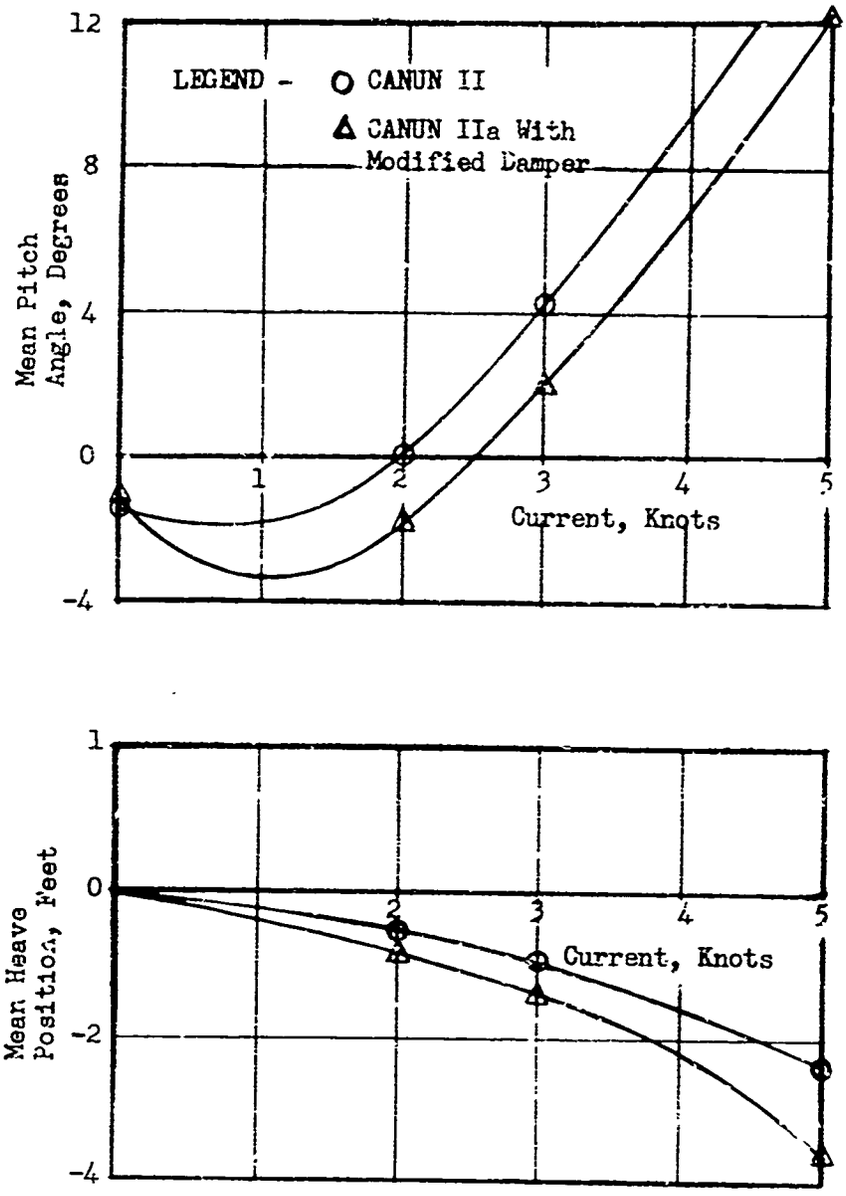

Figure 13. Pitch and Heave Attitude of CANUN II and CANUN IIa Buoys as a Function of Current

8x26 Buoy			
wave ht.	-3 knots	0	+3 knots
Pitch amplitude (degrees)			
2.0	7.2°	7.5°	3.5°
4.0	13.5°	17.1°	9.1°
6.0	16.1°	*	13.1°
Heave amplitude (feet)			
2.0	1.2	1.2	1.0
4.0	2.3	3.0	2.6
6.0	3.0	*	2.6
Surge amplitude (feet)			
2.0	1.2	1.4	0.5
4.0	2.7	2.8	1.0
6.0	3.9	*	1.6

* motions too severe to test

1CR Buoy			
wave ht.	-3 knots	0	+3 knots
Pitch amplitude (degrees)			
2.0	4.4°	1.4°	5.4‡
4.0	9.0°	2.3°	11.6‡
6.0	11.5°	4.0°	9.0
Heave amplitude (feet)			
2.0	0.8	0.9	0.9
4.0	1.8	1.8	1.8
6.0	3.0	2.6	2.4
Surge amplitude (feet)			
2.0	1.1	0.9	0.5
4.0	2.2	1.9	1.3
6.0	3.3	2.8	1.8

‡ heave-roll coupled motions present

Table 6. Variation with Wave Height of Buoy Response in Waves of 5 Second Period

CANUN			
wave ht.	-3 knots	0 speed	3 knots
Pitch amplitude (degrees)			
2.0	4.5°	7.7°	4.9°
4.0	6.3°	15.0°	11.5°
6.0	7.3°	*	15.0
Heave amplitude (feet)			
2.0	0.9	1.1	0.8
4.0	1.9	2.5	2.2
6.0	2.6	*	2.6
Surge amplitude (feet)			
2.0	1.1	0.9	0.4
4.0	2.6	2.0	0.9
6.0	3.4	*	1.3

CANUN II			
wave ht.	-3 knots	0 speed	3 knots
Pitch amplitude (degrees)			
2.0	3.0	10.6°	7.7°
4.0	7.6	26.2°	15.8°
6.0	10.0	*	18.4°
Heave amplitude (feet)			
2.0	1.0	1.1	1.0
4.0	2.1	3.0	1.8
6.0	2.7	*	2.6
Surge amplitude (feet)			
2.0	1.2	0.9	0.5
4.0	2.5	1.8	1.0
6.0	3.8	*	1.4

* motions too severe to test

Table 6 (cont'd.) Variation with Wave Height of Buoy Response in Waves of 5 Second Period

CANUN IIa Buoy		
wave ht.	0 speed	+3 knots
Pitch amplitude (degrees)		
2.0	6.3°	7.4°
4.0	14.1°	10.2°
6.0	17.6	12.9
Heave amplitude (feet)		
2.0	1.1	0.5
4.0	2.5	1.6
6.0	3.7	2.0
Surge amplitude (feet)		
2.0	1.0	0.5
4.0	2.0	0.8
6.0	2.7	1.3

Table 6 (cont'd.) Variation with Wave Height of Buoy Response in Waves of 5 Second Period

Section 7

BUOY PITCH PERFORMANCE IN A RANDOM SEAWAY

In order to ascertain the visibility of the various buoys tested, it is necessary to determine the percentage of the time that the buoys are near enough to the vertical, so that the light or radar reflector can be seen at great distances. For this purpose, we will determine the expected percentage of time that each of the buoy configurations is with 2°, 3° and 4° of the vertical.

To perform this analysis, it is necessary to determine their pitch and roll response in a random seaway. As mentioned in the previous section, the roll motions experienced during the tests of the buoys in unidirectional, regular waves were the result of non-linear effects such as heave-roll instabilities, wandering, etc. With the current state-of-the-art, it is impossible to incorporate these second-order effects in a rational, predictive procedure. The roll motions will not, therefore, be considered explicitly here. It is to be noted that these effects are less likely to take place in the open ocean where the waves come from all different directions and are composed of a spectrum of different wave lengths and frequencies. Here, the motions are never steady and the time required for the several instabilities to build up does not exist. The significant roll motions are likely to be induced by waves travelling at a direction different than the current direction. In the tests reported herein, no tests were made with the waves and current in other than coincident directions. As a result, only the pitch motions are considered. Roll motions will serve to degrade the percentage of time that a buoy is a certain number of degrees to the vertical compared to the same percentage calculated from the pitch motions only.

It is felt, however, that the results are indicative of the trends to be expected in the ocean.

7.1 THE ANALYSIS

It will be assumed that the seaway can be described in terms of a Neumann wave spectrum given by:

$$A^2(\omega) = C\omega^{-6} \exp\left[-2g^2/(\omega V_w)^2\right] \qquad (1)$$

where

C = 51.5 ft^2/sec^5, a constant
V_w = wind velocity, ft/sec
ω = wave frequency, radians/sec
g = gravitational acceleration, 32.2 ft/sec^2
$A^2(\omega)$ = the height^2 of the wave component of frequency ω, per unit ω.

If $\theta(\omega)$ is the response amplitude operator of the buoy (in this case, the pitch angle amplitude of the buoy for one foot amplitude wave, as a function of ω), then the root mean square pitch motion in the seaway is given by

$$\sigma_\theta = \left\{\tfrac{1}{2}\int_0^\infty \theta^2(\omega)\, A^2(\omega)\, d\omega\right\}^{\frac{1}{2}} \qquad (2)$$

During the current test program, only six values of $\theta(\omega)$ were determined for any buoy configuration and current condition. With only these few points, it is impossible to perform the integration indicated in (2) accurately. As a result, the following procedure was adopted.

It is well known that all floating objects exhibit a pitch motion equal to the wave slope for waves which are very long compared to any of the

object's dimensions. Thus, if $S(\omega)$ is the maximum slope of a unit amplitude wave, then

$$\lim_{\omega \to 0} \frac{\theta(\omega)}{S(\omega)} = 1 \tag{3a}$$

Further, it is known that

$$\lim_{\omega \to \infty} \frac{\theta(\omega)}{S(\omega)} = 0 \tag{3b}$$

In between these two limiting frequencies the object generally behaves like a second-order oscillator defined by a natural frequency and damping ratio. Here

$$\frac{\theta(\omega)}{S(\omega)} = \frac{1}{\left[\left(1 - \frac{\omega^2}{\omega_n^2}\right)^2 + 4\zeta^2 \frac{\omega^2}{\omega_n^2}\right]^{1/2}} \tag{4}$$

where

ω_n is the natural frequency

ζ is the damping ratio.

It is reasonable to expect that the buoy will behave in a similar fashion. Therefore, for each buoy configuration and current combination, the wave slope corresponding to each wave frequency was computed and the pitch amplitude response divided by that wave slope. This computed wave slope included the effects of the finite depth of water. A least-squares fit to these normalized responses was made with the second order oscillator function given in (4). The resulting natural frequency and damping ratio were used, together with (4) to perform the integration indicat in (2). It is assumed that the pitch motion has a Gaussian distribution.

The probability that the buoy is within α of the vertical can, therefore, be expressed as

$$p(\omega) = f\left(\frac{\alpha - \theta_m}{\sigma_\theta}\right) - f\left(\frac{-\alpha - \theta_m}{\sigma_\theta}\right) \qquad (3)$$

where

$f(x)$ is the nomalized cummulative probability function of x

θ_m is the mean pitch angle (presented in section 6.4)

The probability thus computed represents the expected fraction of time the buoy is between the limits $\{-\alpha, \alpha\}$.

7.2 RESULTS

The above technique was used to analyse the pitch response data presented in Tables 1-5. The natural frequency and damping ratios of equivalent second-order oscillators were determined and the root-mean-square pitch amplitude in five seaways were computed. The following Table lists the five values of the wind velocity, V_w, used in equation (1) and the corresponding approximate sea state.

V_w(knots)	Sea State	Signif. Wave Ht.
10	2-	1.4
12	2+	2.2
14	3	3.3
16	3+	4.6
18	4	6.1

The rms values of pitch amplitude, together with the mean pitch angles were used in equation (3) to determine the probability that the buoy is within 2^o, 3^o and 4^o from the vertical. The results are presented

in figures 14 through 18. The following sections discuss the results for each buoy in detail.

7.2.1 The 1CR Buoy (figure 14).

It is seen that the rms pitch amplitude of the buoy increases uniformly with sea state for each of the current combinations. The distinction between the pitch motions for the different current conditions and the two mooring locations (0 and $\pm$ 2 knots the buoy was moored at the bottom eye, $\pm$ 3 knots the buoy was moored on the current bar) is not dramatic. We see, however, that the difference between the different mooring locations is very important in the percentage of time that the buoy is vertical.

At zero knots, the mean buoy angle is near zero and, as a result, the fraction of time that the buoy is near vertical decreases in proportion to the rms pitch amplitude. That is, this percentage of time decreases uniformly with increases of sea state.

The 2° angle limit produces a smaller probability than the 3° limit which in turn is smaller than the 4° limit. This is to be expected, of course, since the 4° limit completely contains the 3° limit and 2° limit.

The results for the 2 knot condition are dramatically different than those for the 0 knot condition. The percentage of time that the buoy is within the angle limits grows with increasing sea state. This occurs because the mean pitch is larger than any of the angle limits. When there is no motion (sea state 0), the fraction of time it is near vertical is zero. As the sea state and thus, motion increases, the chance that the pitch angle is within the limits increases. At high enough sea states, the probability will again decrease since the motions will be so much larger than the interval between the limits.

The results for the ± 3 knot current lie somewhat between the 0 and ± 2 knot conditions. Again, this is chiefly because of the mooring induced static pitch angles which were larger than the zero knot condition and less than the ± 2 knot condition. Because the mean pitch angle is closer to zero than the ± 2 knot cases, the rise and decrease of the fraction of time is more pronounced than the 2 knot case.

7.2.2 The 8x26 Buoy (figure 15).

Unlike the 1CR, the results for the 8x26 buoy vary consistently with increases in speed and sea state. This is because the mooring system does not change. In general, we see that the rms pitch amplitudes tend to decrease in a current for a given sea state and increase with sea state for a given current. Because of the increasing mean pitch angle with current, the fraction of time that the buoy remains near vertical is smaller with increasing pitch angle.

7.2.3 The CANUN Series

7.2.3.1 The CANUN Buoy (figure 16).

The mooring arrangement used for the CANUN buoy resembled that of the 1CR buoy. For currents of 0 and ± 2 knots, the bottom eye was used. At ± 3 knots, the 2nd hole from the bottom on the current bar was used. As a result, the mean pitch angle at ± 2 knots was considerably more than that at either zero knots or ± 3 knots. Qualitatively, the fractional time results are similar to the 1CR buoy.

7.2.3.2 The CANUN II Buoy (figure 17).

Here, the single point moor greatly reduced the range of the mean pitch angles. Because the pitch damping was less for this configuration, the

rms pitch amplitudes were greater than for the CANUN. Over the whole range of currents, however, the fractional time within the various angle limits is more than the CANUN configuration.

7.2.3.3 The CANUN IIa Buoy (figure 18).

The addition of the pitch damper produced substantially smaller rms pitch amplitudes than the CANUN II and had a similar variation of the mean pitch angle as the CANUN II. Thus, the fractional time within the pitch angle limits is more for this buoy. In fact, in comparison with the other buoys tested, the predictions show that this buoy will remain upright the greatest percentage of time.

7.2.4 Conclusion

It can be seen from the above figures that the single most important variable governing the fractional time the buoy is within the pitch limits is the mean pitch angle. It is only when the mean pitch angle itself is small that the magnitude of the motions becomes dominant.

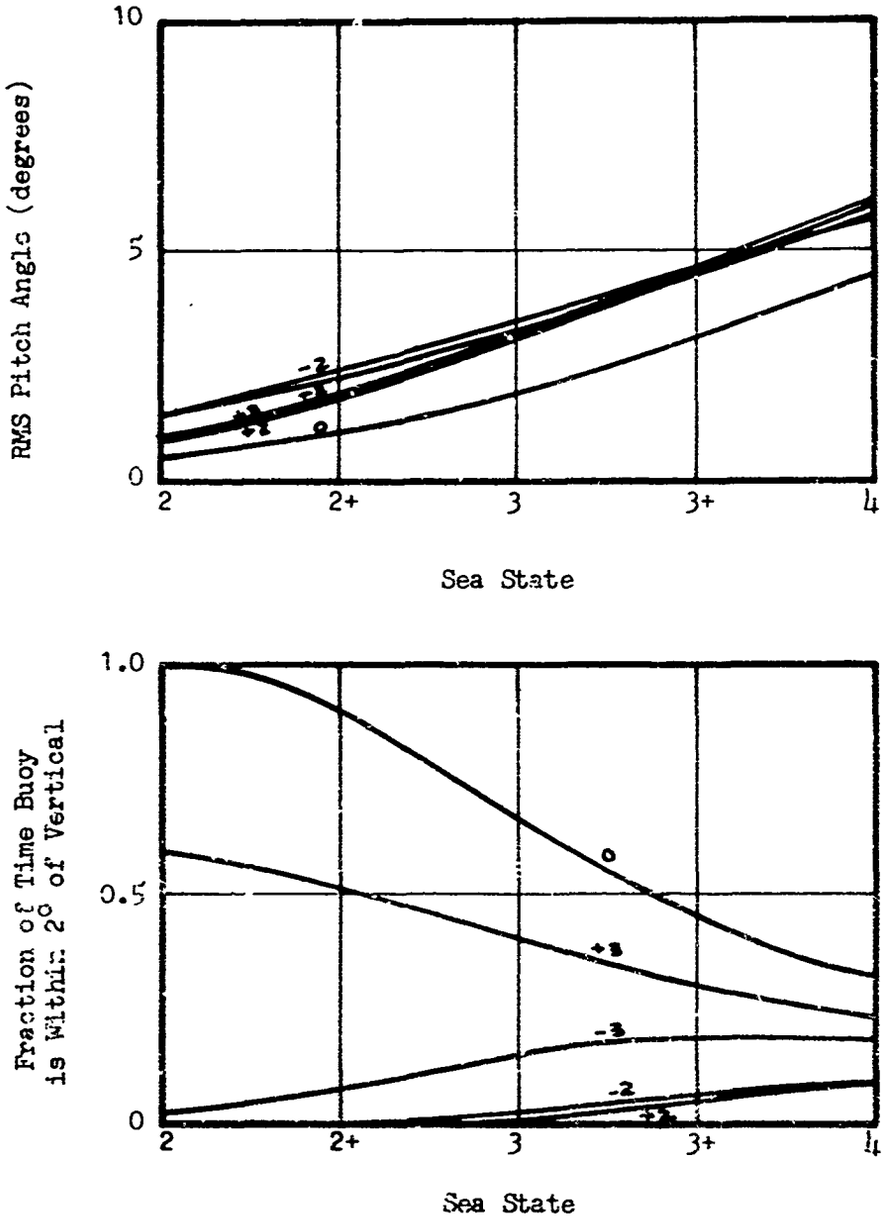

Figure 14. The Root-Mean-Square Pitch Amplitude and Fractional Time with 2, 3 and 4° of vertical as a Function of Sea State - 1CR Buoy

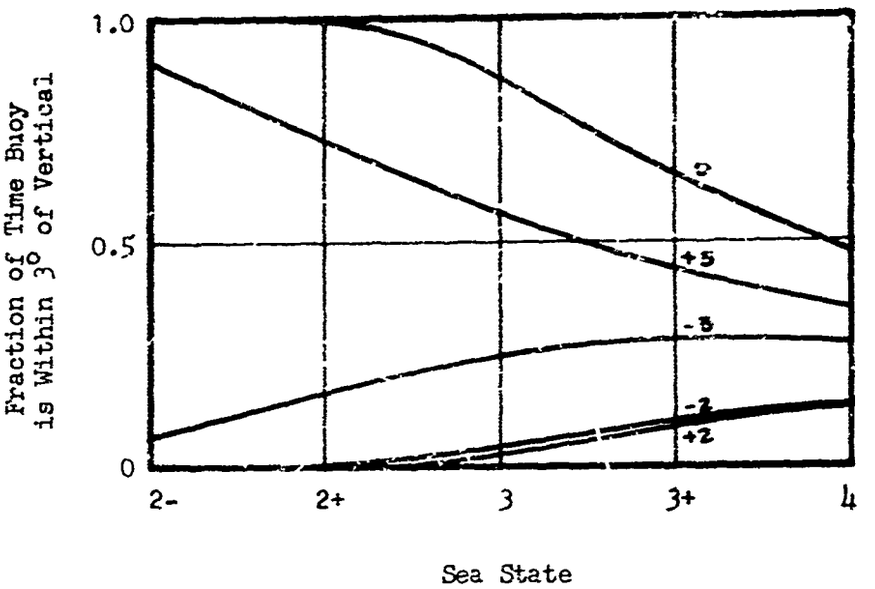

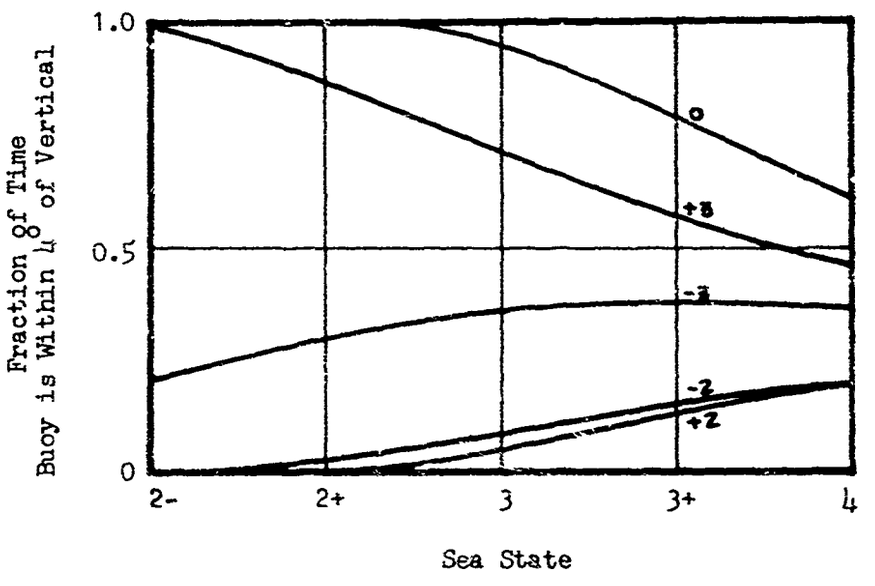

Figure 14 (Cont'd). 1CR Buoy

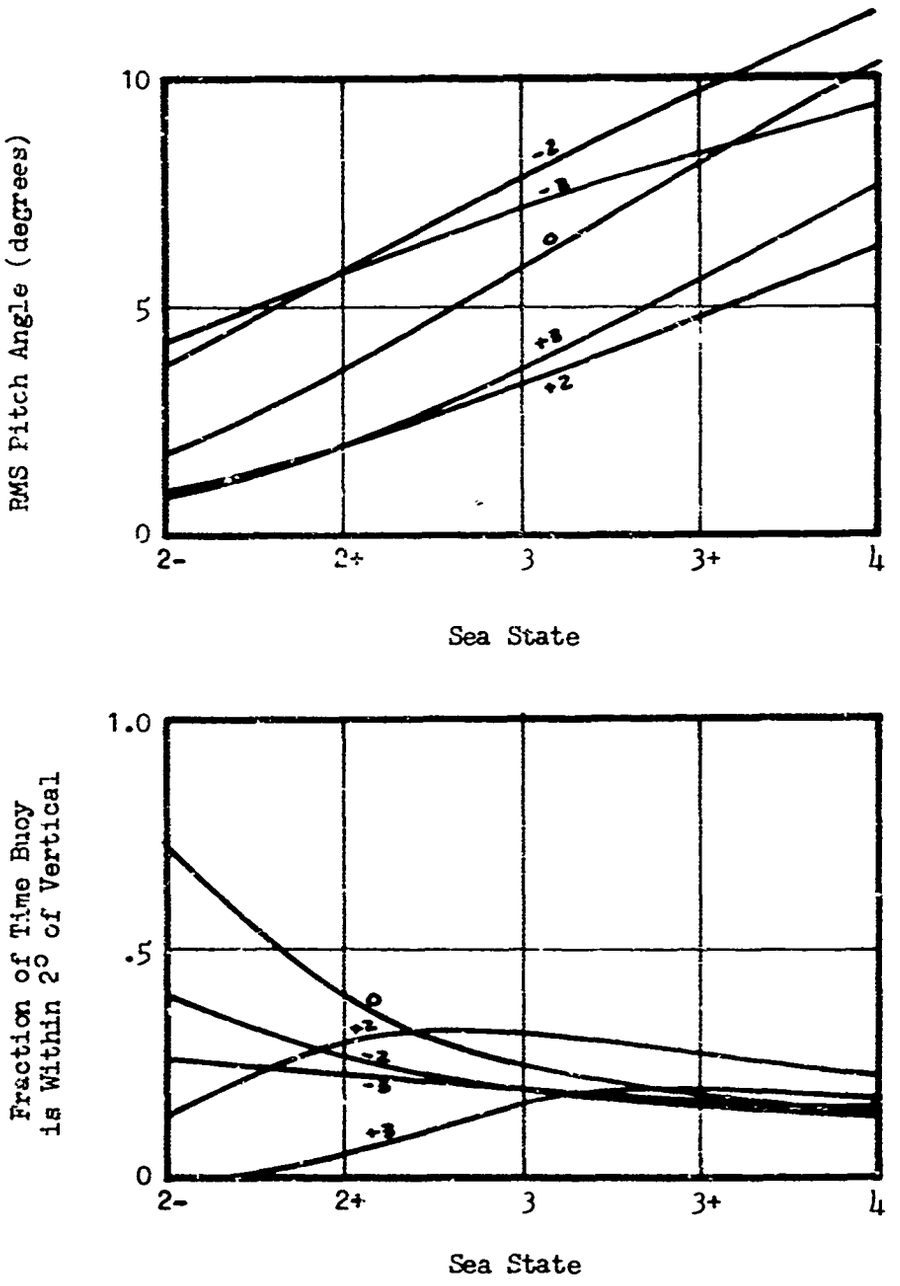

Figure 15. The Root-Mean-Square Pitch Amplitude and Fractional Time with 2, 3 and 4° of Vertical as a Function of Sea State - 8x26 Buoy

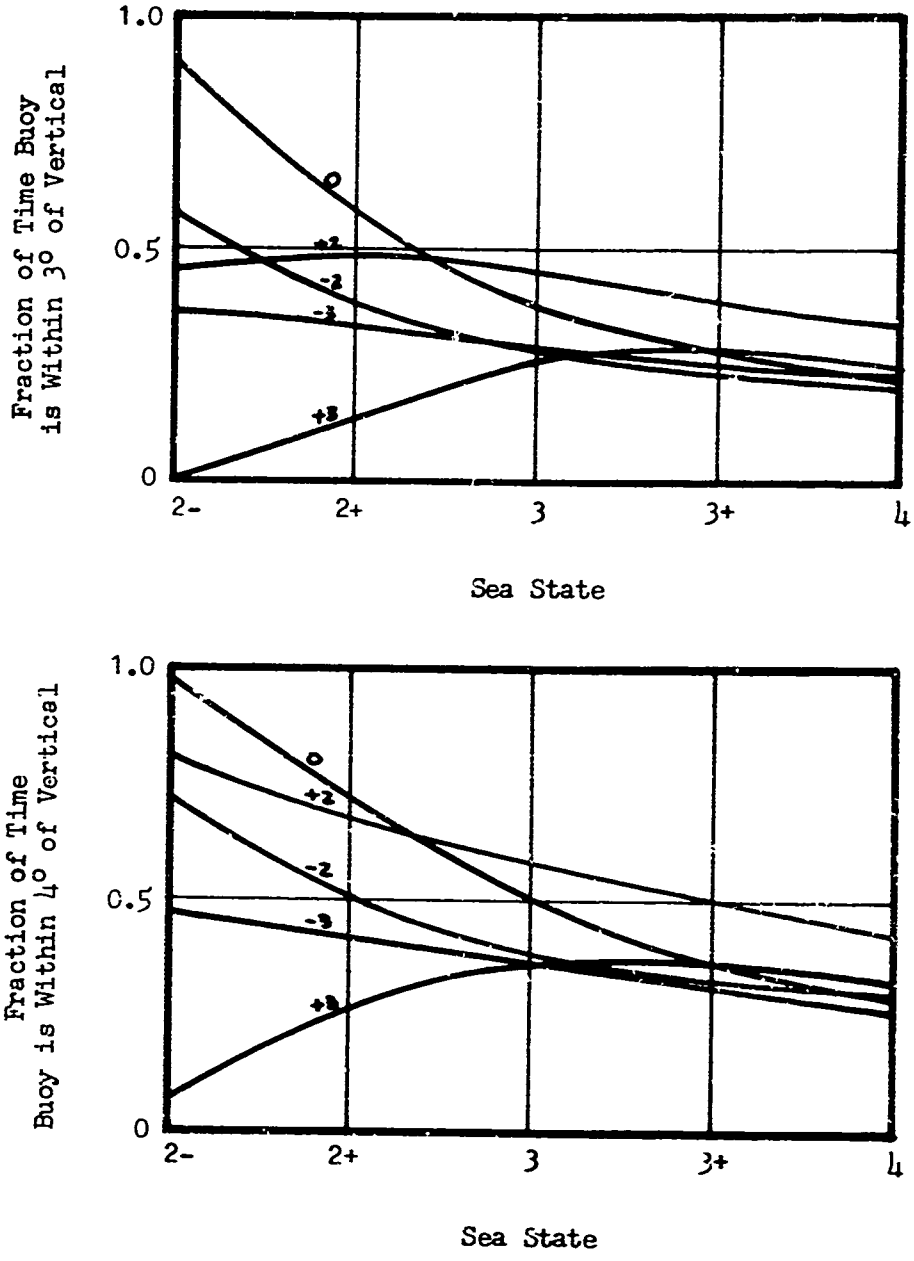

Figure 15 (Cont'd). 8x26 Buoy

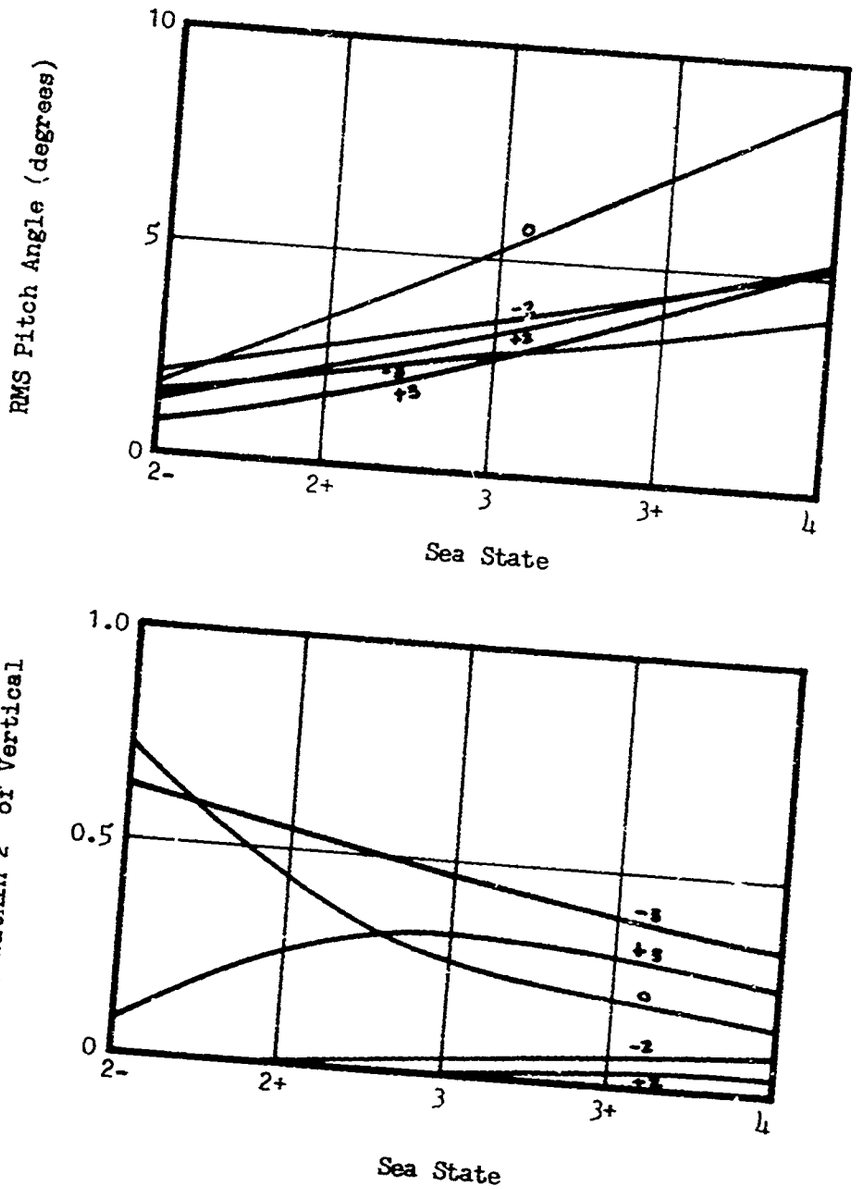

Figure 16. The Root-Mean-Square Pitch Amplitude and Fractional Time with 2, 3 and 4° of Vertical as a Function of Sea State - CANUN Buoy

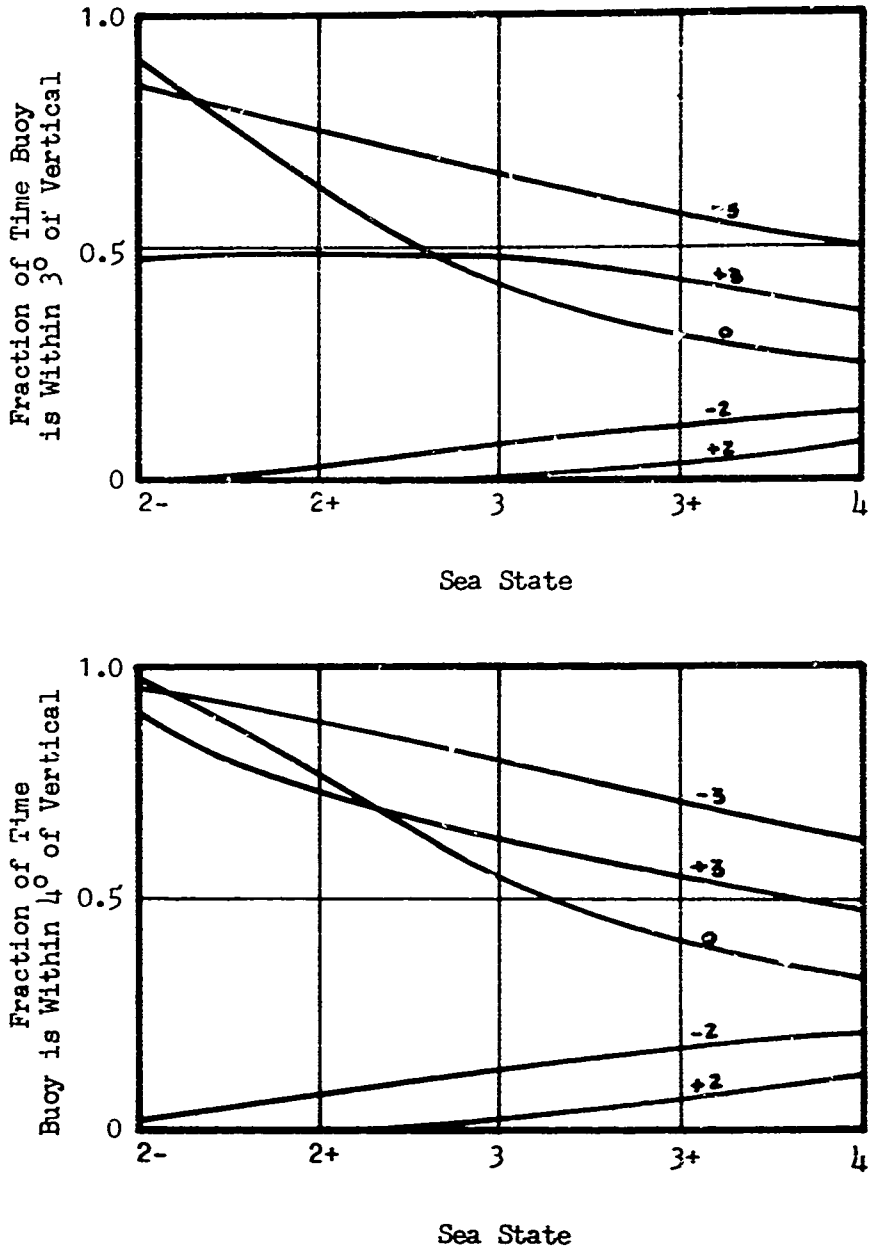

Figure 16 (Cont'd). CANUN Buoy

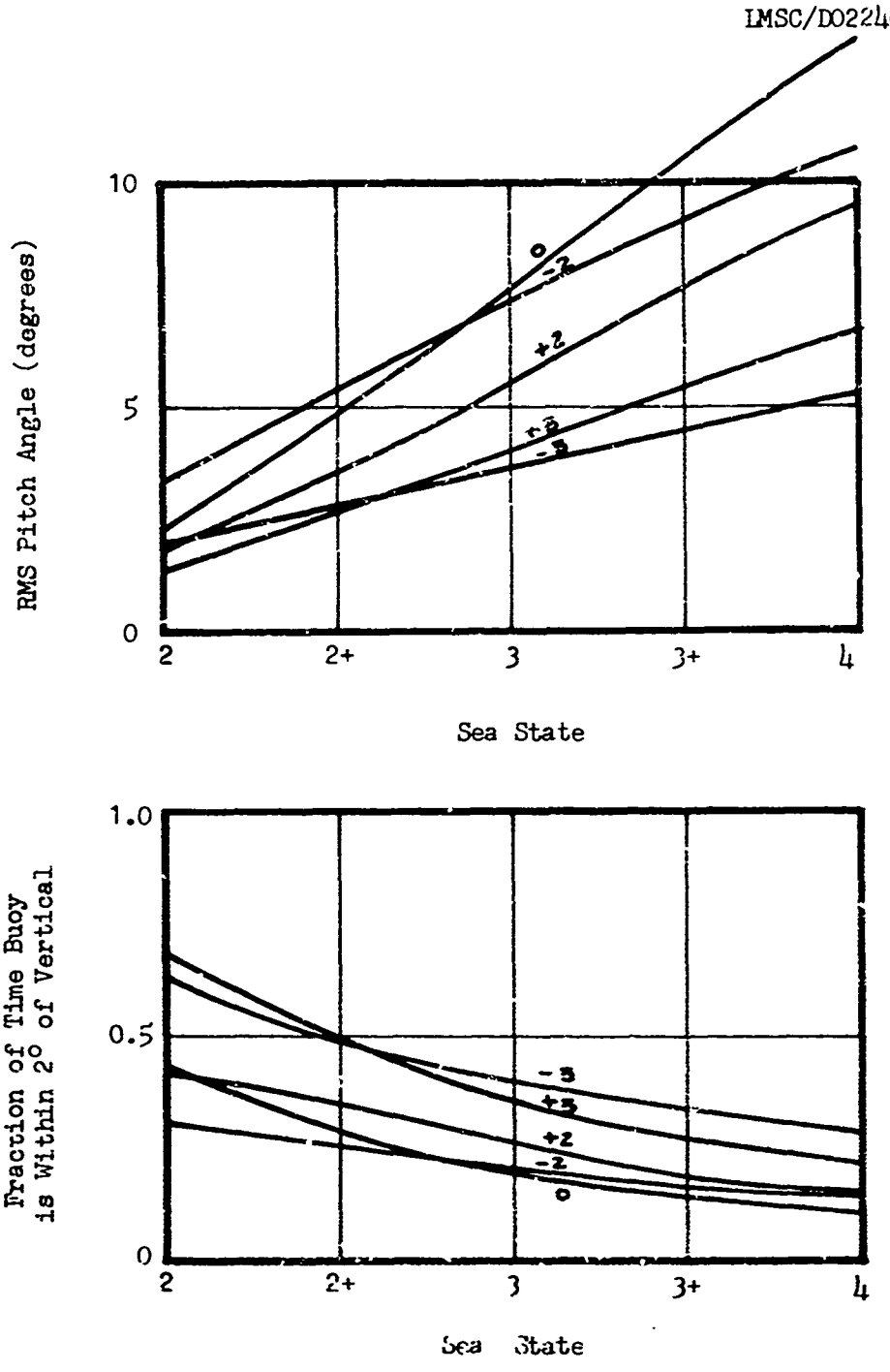

Figure 17. The Root-Mean-Square Pitch Amplitude and Fractional Time with 2, 3 and 4° of Vertical as a Function of Sea State - CANUN II Buoy

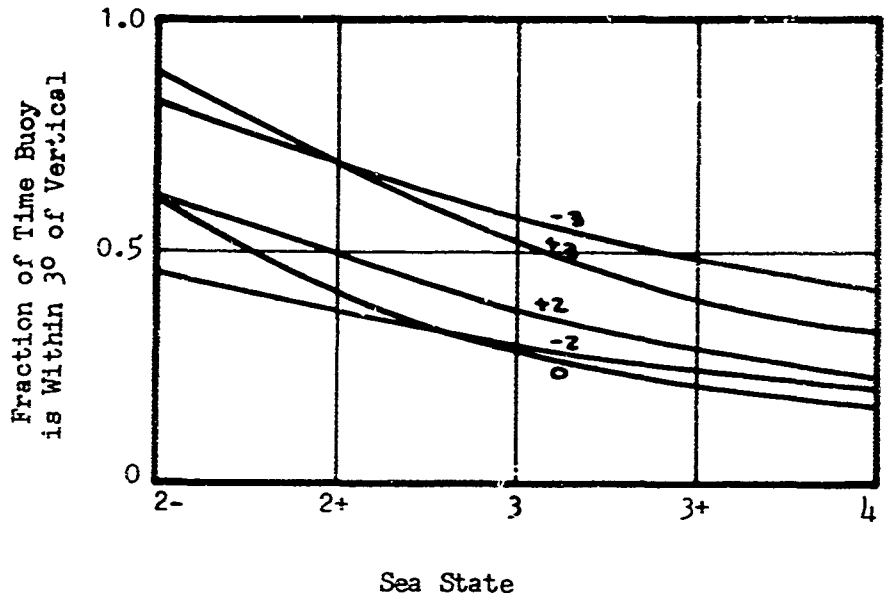

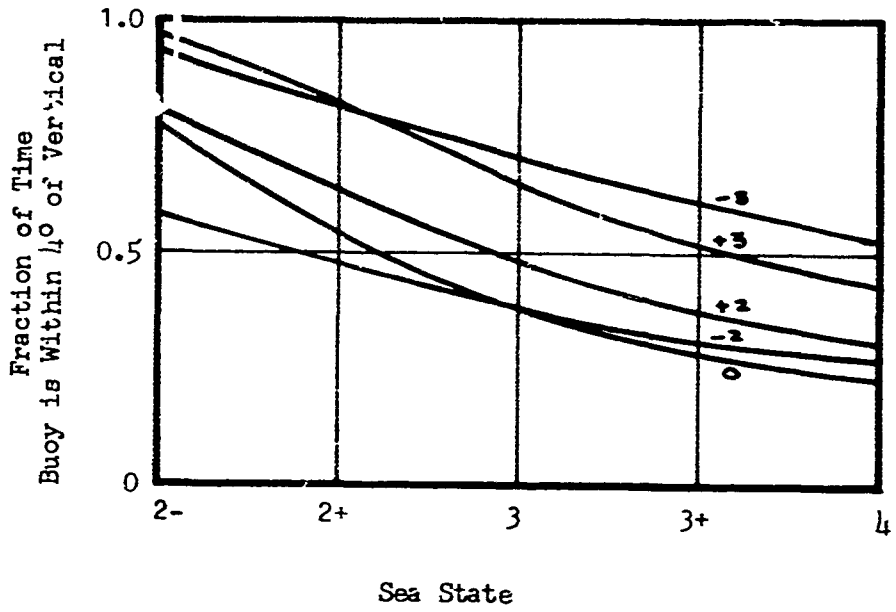

Figure 17 (Cont'd). CANUN II

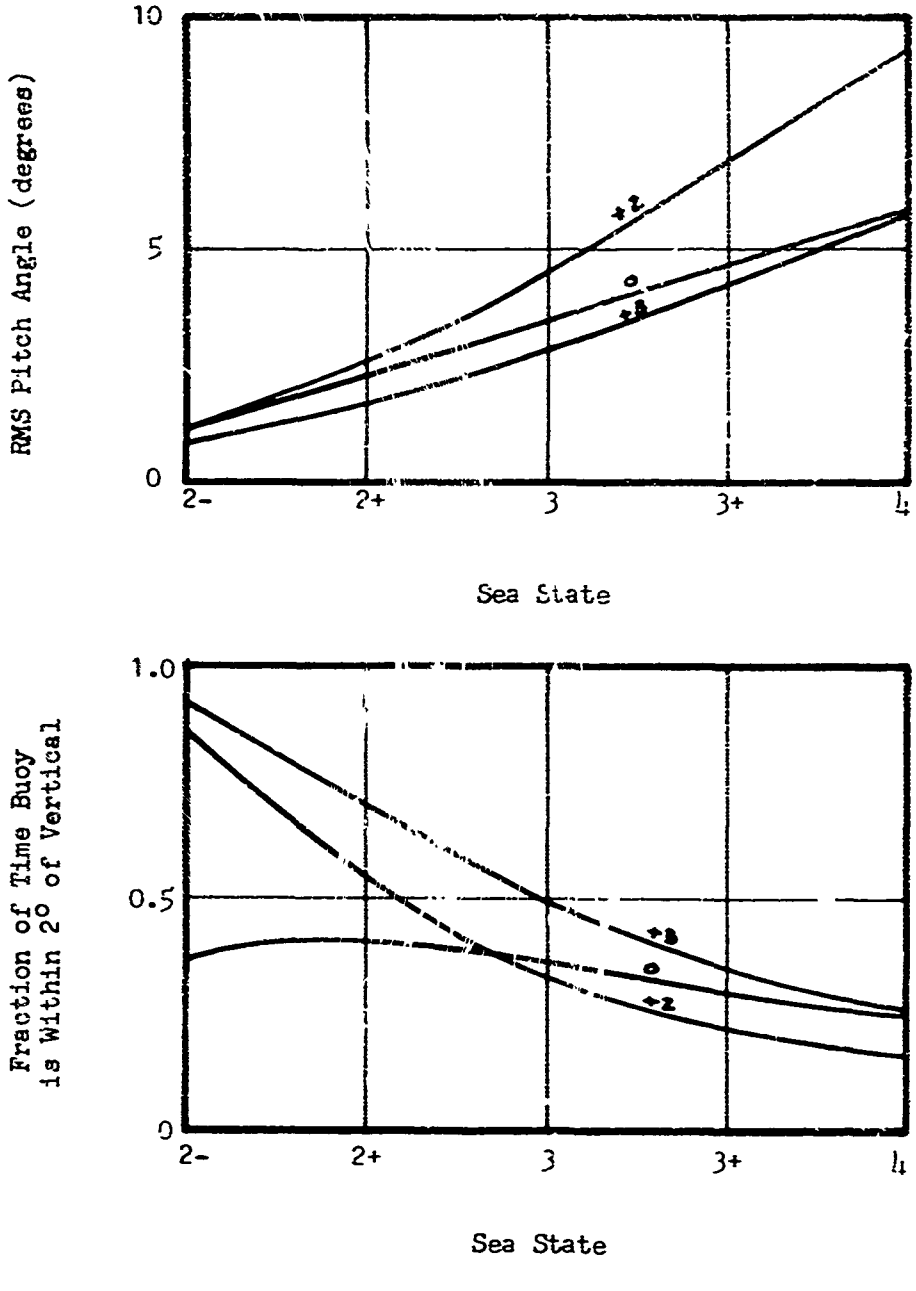

Figure 18. The Root-Mean-Square Pitch Amplitude and Fractional Time with 2, 3 and 4° of Vertical as a Function of Sea State - CANUN IIa Buoy

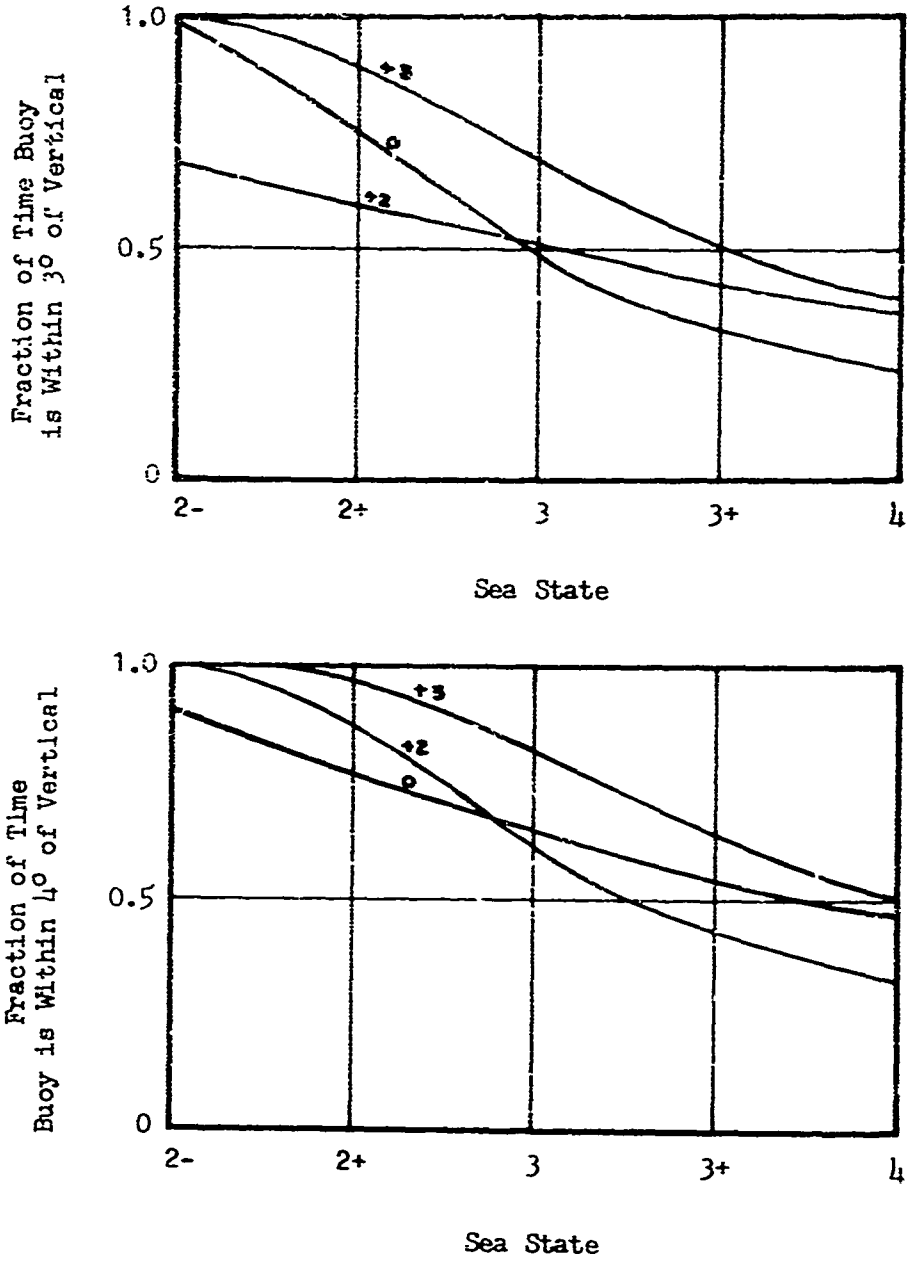

Figure 18. (Cont'd). CANUN IIa Buoy

Section 8

CONCLUSIONS

On the basis of the tests that were performed we reached the following conclusions:

1. All of the buoys tended to wander in a direction normal to the current. This wandering was random and is apparently due to vortex shedding by the buoy. Whenever the buoy was moored on a current bar, the wandering was greatly worsened and accompanied by severe yaw motions.

2. Roll motions were experienced only as a result of the wandering or various second-order effects. These effects included heave-roll instabilities and pitch-roll coupled motions. The roll motion induced by wandering was random in character. Otherwise, very little roll motion was experienced.

3. The pitch motions of all the buoys appeared to have a sharp resonant peak at wave periods corresponding to the measured pitch resonance. Heave motions demonstrated, in general, a slight resonance, and surge motions almost none. The effect of current generally diminished all of these motions somewhat.

4. The average pitch angle was greatly affected by the exact mooring configuration. The use of a bottom eye to moor gives rise to small mean pitch angles at zero speed, and rather large mean pitch angles at small currents. Conversely, the current bar leads to large mean pitch angles at zero speed and small mean pitch angles at small

currents. Only the bridal and single point mooring systems had relatively small mean pitch angles throughout the current range. Of the two, the single point moor had the smallest mean pitch angles.

5. The 1CR buoy and CANUN buoy tended to sink deeper in the water with increasing current. This was apparently caused by the downward component of the chain load, which also increased with current. The 8x26 buoy rose slightly and there is evidence that this was caused by planing on the bottom dome of the buoy. It is expected, however, that at currents of higher speeds than were tested that the planing effect could be diminished.

6. The mean surge position appeared to increase more or less linearly with the speed of the current. Although one could expect the buoy drag to grow quadratically with the current speed, the restoring force of the chain grows exponentially with its displacement. These two effects appeared to balance each other within the range of currents tested.

7. The most important single factor governing the fractional time that the buoy is near vertical appears to be the mean pitch angle. Only if the mean pitch angle is small, does the magnitude of the pitch motions become important.

8. The CANUN IIa had the best visibility characteristics over all seaway and current conditions; the 1CR and CANUN had the worst characteristics. For the CANUN IIa, the fractional time that the buoy remains within the pitch limit decreased uniformly with increasing sea state and was never less than 32% up to sea state 4 for the $\pm 4^{\circ}$ limit.

Appendix A

ANALYSIS FOR GYRADIUS EXPERIMENT

Appendix A

ANALYSIS FOR GYRADIUS EXPERIMENT

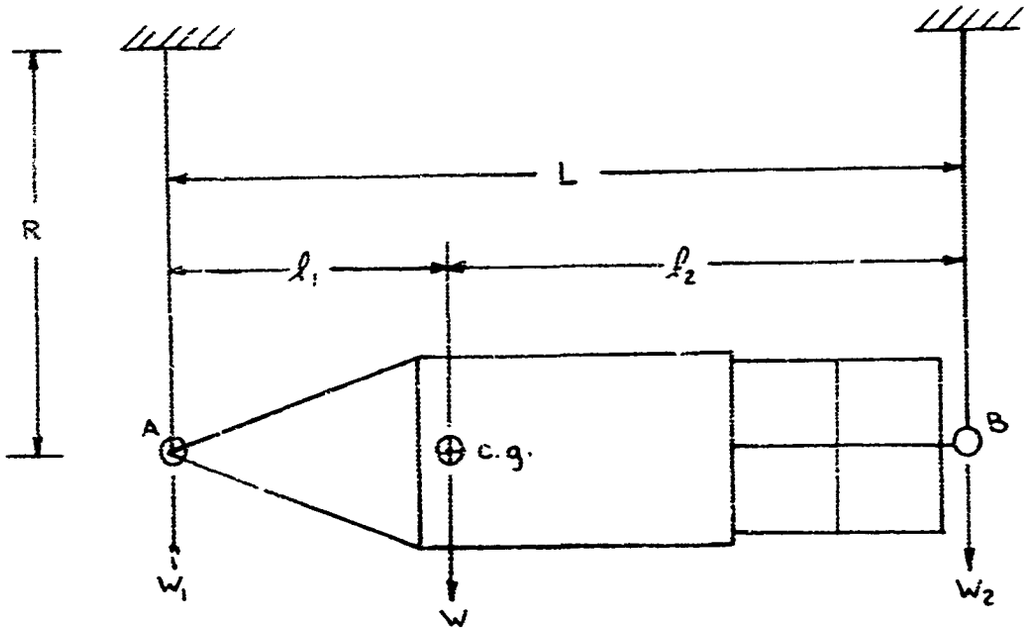

$$W = W_1 + W_2,\ W_1 = \frac{\ell_2 W}{L},\ W_2 = \frac{\ell_1 W}{L}$$

For a angular displacement θ about the c.g. we have a displacement $\ell_1\theta$ about point A & a displacement of $\ell_2\theta$ about point B. These displacements cause a restoring force of approximately $\frac{W_1 \ell_1 \theta}{R}$ at point A and $\frac{W_2 \ell_2 \theta}{R}$ at point B. Thus the total restoring moment is given by:

$$\mathcal{M} = \ell_1 \cdot \frac{W_1 \ell_1 \theta}{R} + \ell_2 \cdot \frac{W_2 \ell_2 \theta}{R}$$

$$= \ell_1 \ell_2 (\ell_1 + \ell_2) \frac{W\theta}{RL} = \ell_1 \ell_2 \frac{W\theta}{R}$$

The equation of motion is (neglecting damping) is given by

$$I\ddot{\theta} + \ell_1 \ell_2 \frac{W\theta}{R} = 0$$

but

$$I = \frac{Wr^2}{g}, \text{ where r is the gyradius}$$

Thus,

$$\frac{Wr^2\ddot{\theta}}{g} + \ell_1 \ell_2 \frac{W\theta}{R} = 0$$

and

$$\omega_m = \sqrt{\frac{\ell_1 \ell_2 g}{R r^2}}$$

or

$$T = 2\pi r \sqrt{\frac{R}{\ell_1 \ell_2 g}}$$

and

$$r = \frac{T}{2\pi} \sqrt{\frac{\ell_1 \ell_2 g}{R}} \simeq 0.90312T \sqrt{\frac{\ell_1 \ell_2}{R}}$$

Thus, to measure the gyradius, it is only necessary to measure ℓ_1, ℓ_2, R and the period of pendulation. The above formula is then used to obtain the gyradius.

Appendix B

LOCKHEED UNDERWATER MISSILE FACILITY

LOCKHEED UNDERWATER MISSILE FACILITY

The Lockheed Underwater Missile Facility is a large cross-section wave channel and test basin with variable atmospheric pressure. A high speed towing system is installed on the wave channel. Figure B-1 is a sectional drawing of the general arrangement of the facility.

Wave Channel and Test Basin

The wave channel and test basin is a rectangular, reinforced concrete tank with interior wall dimensions of 180 ft. long by 15 ft. wide. Allowing a 2-foot free board for waves, the standard water depth in the wave channel is 15 feet resulting in 25 and 35 foot deep water in the test basins. The 37 feet deep basin is equipped with an elevating platform which supports missile launching or other special test equipment weighing up to 7000 lbs. The 27 feet deep basin is 40 ft. long, and when used with the adjacent deep basin provides an unobstructed basin 56 feet long with 25 feet of water. Eleven underwater optical viewing ports, 20 inches square, are flush mounted in one wall in the region of the deep basin. The wave channel is filled with fresh water.

Wave Generator and Beach

The wave channel is equipped with a 17 feet high, piston-type wave generator which spans the tank 14 feet from the west end. Wave heights up to 2.35 feet, crest-to-trough, can be generated. Wave periods can be varied from 0.8 to 4.8 seconds, producing wave lengths from 3.8 to 91 feet. A wave absorbing beach is provided at the opposite end of the channel. The 14 degree sloping face of the beach extends 21 feet into the tank, at which point it is truncated by a vertical face extending nearly to the floor of the channel. The beach is composed of two layers of 2 feet thick stainless steel baskets filled with stainless steel turnings on both the sloping and vertical beach faces.

Pressure Shell

The wave channel is largely enclosed in a 27½ ft. diameter, horizontal, cylindrical pressure vessel. The vessel is structurally capable of withstanding complete evacuation. The walkway and work area around three sides of the tank are enclosed within the shell allowing access to the edge of the channel. Evacuation of the facility is accomplished with three, single-stage, 50 hp vacuum pumps which are installed in parallel. There are two large (10 by 10 feet) equipment hatches located in the top of the shell over the deep pits. Two smaller (36 by 36 inch) hatches in the 10 foot hatches are used for regular handling of test models and small equipment. A traveling crane is installed over the hatch area for handling of this equipment.

Towing System

The towing system, shown in Fig. B-2, is installed on the top of the walls of the wave channel. This system is composed of a rigid steel carriage which rides on Fiberglas wheels on a pair of ground steel rails. The carriage, shown in Fig. B-3, is 9 feet long, 17 feet wide, by 36 inches high and weighs approximately 12,000 pounds. The carriage speed is adjusted and maintained by servo controlled hydraulic motors mounted on the carriage and geared through a single spur gear against a gear rack. A trailing system provides continuous direct connection of power, air, controls and instrumentation to the towing carriage. Test equipment weighing up to 1200 pounds may be installed on the carriage. A six-component balance for measuring forces up to 1000 pounds may be installed on the carriage.

Physical characteristics and capabilities of the facility are presented in Fig. B-4.

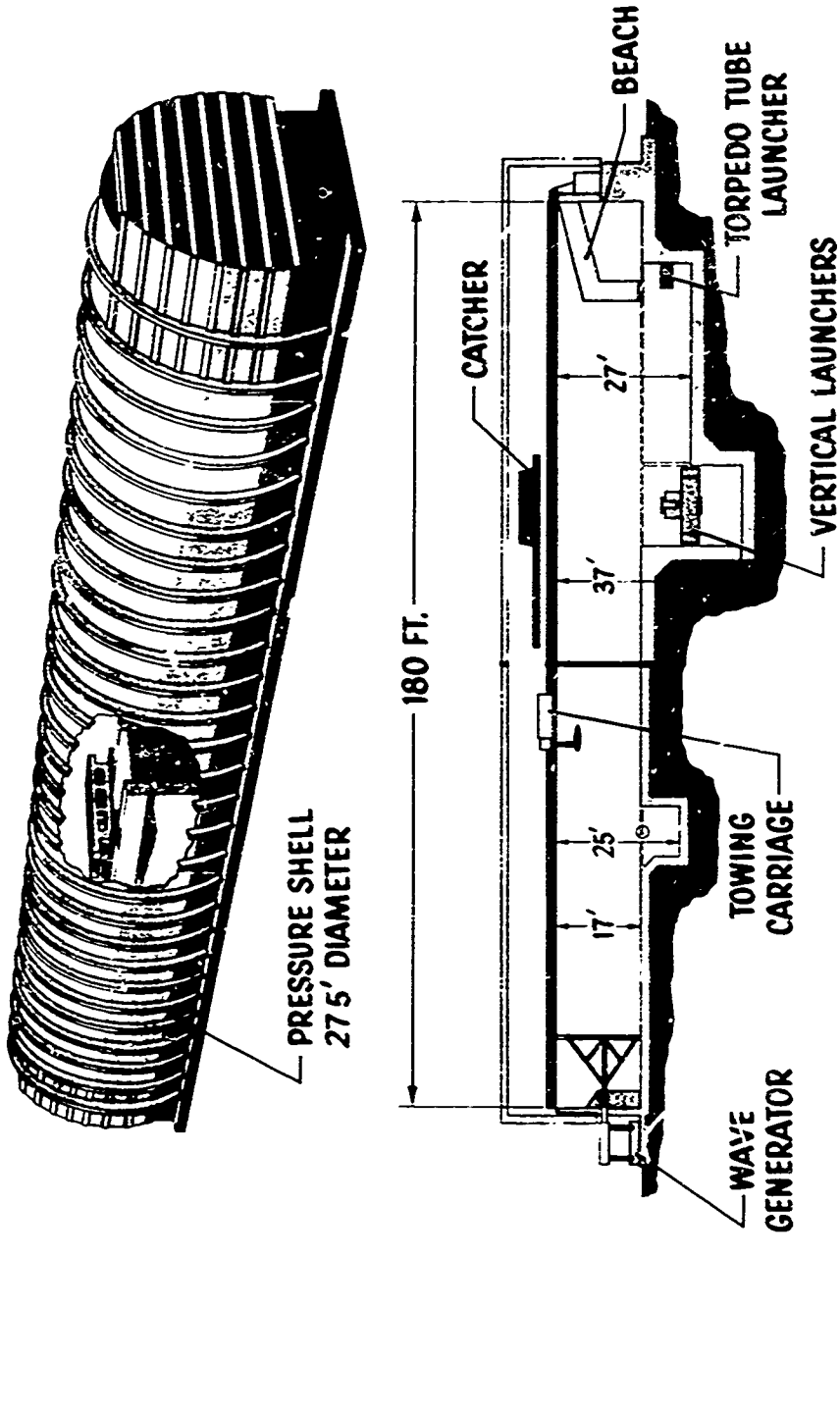

Fig. B-1 General Arrangement of LUMF

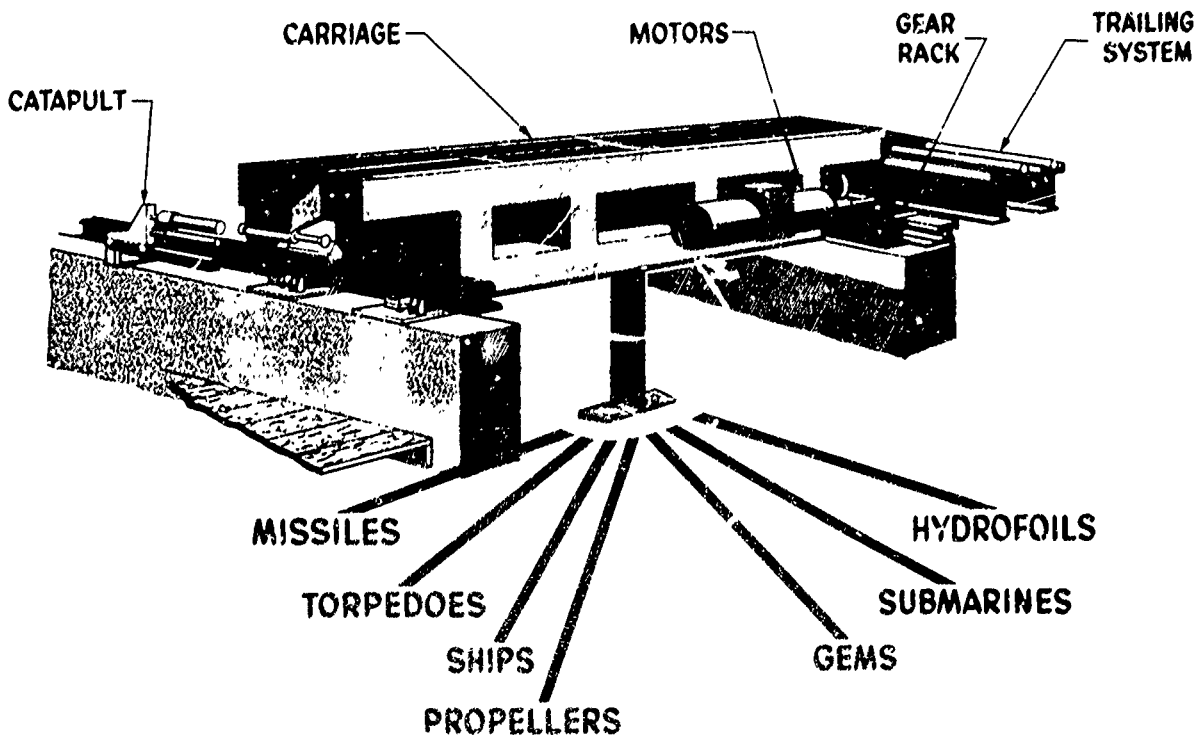

N 8364 10/24/62

LOCKHEED MISSILES and SPACE COMPANY

Fig. B-2 LUMF Towing System

Fig. B-3 LUMF Towing System Installed

WATER CHANNEL

Length	180 feet
Width	15 feet
Depth	15 feet minimum
	25 feet pit
	35 feet deep pit

Water temperature 60°F ± 7°F

FORCE BALANCE

Number of components	6
Nominal range: lift	± 1000 lbs
drag	± 500 lbs
sideforce	± 1000 lbs
pitch	± 15,000 in-lbs
roll	± 10,000 in-lbs
yaw	± 12,000 in-lbs
Accuracy estimated	± 0.1% full scale

VAPOR CAVITATION NUMBER

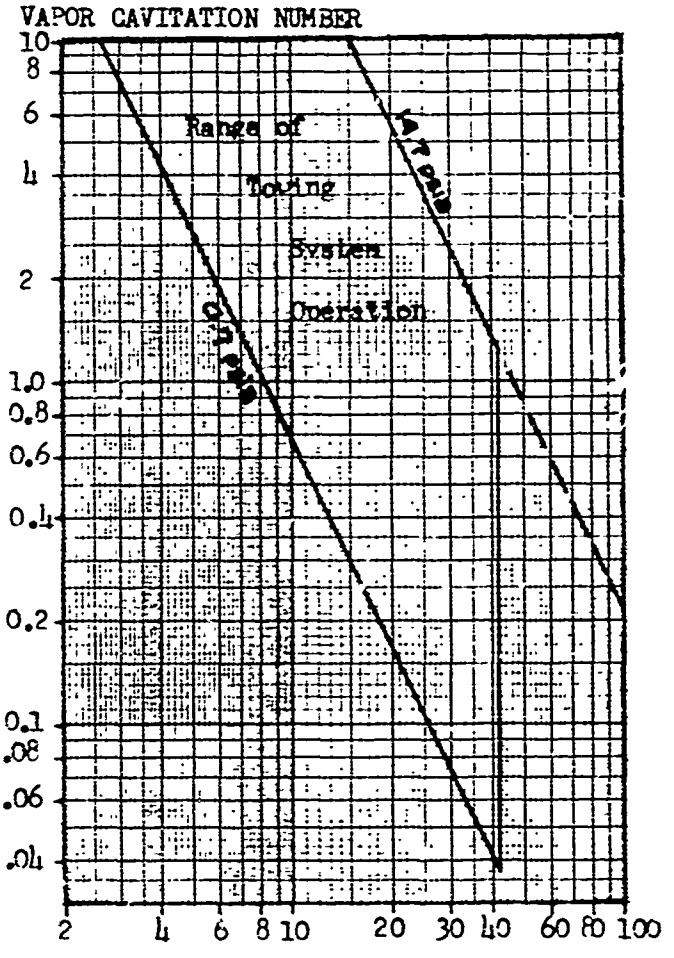

Test Velocity - feet per second

WAVES

Height	0.1 to 2.35 feet crest-to-trough
Period	0.8 to 4.8 seconds
Length	3.8 to 91 feet

TOWING SYSTEM

Speed	2 to 42 ft/sec
Speed variation	± 0.5% of mean
Catapult acceleration	44 ft/sec^2

Run time - seconds

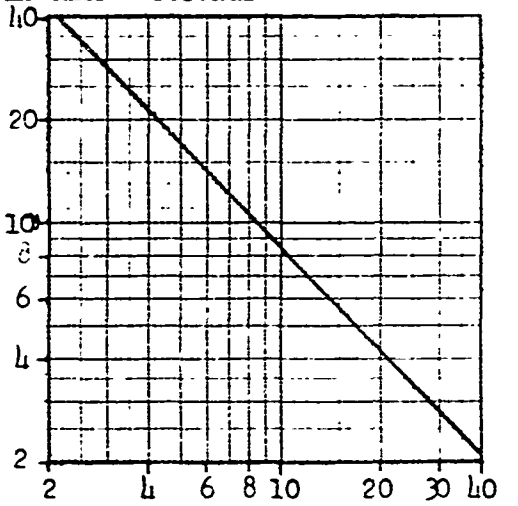

Test Velocity--feet per second

CONTROLLED AIR PRESSURE

Range 0.7 to 14.7 psia

Pressure - psia

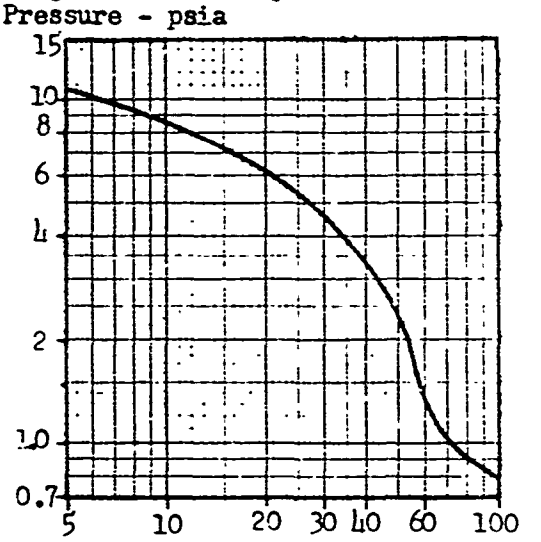

Time to Acquire Pressure -- minutes

Fig. B-4 LUMF Physical Characteristic and Capabilities

Appendix C

DEVELOPMENT OF THE SINGLE POINT MOORING SYSTEM

Appendix C

Development of the Single Point Mooring System

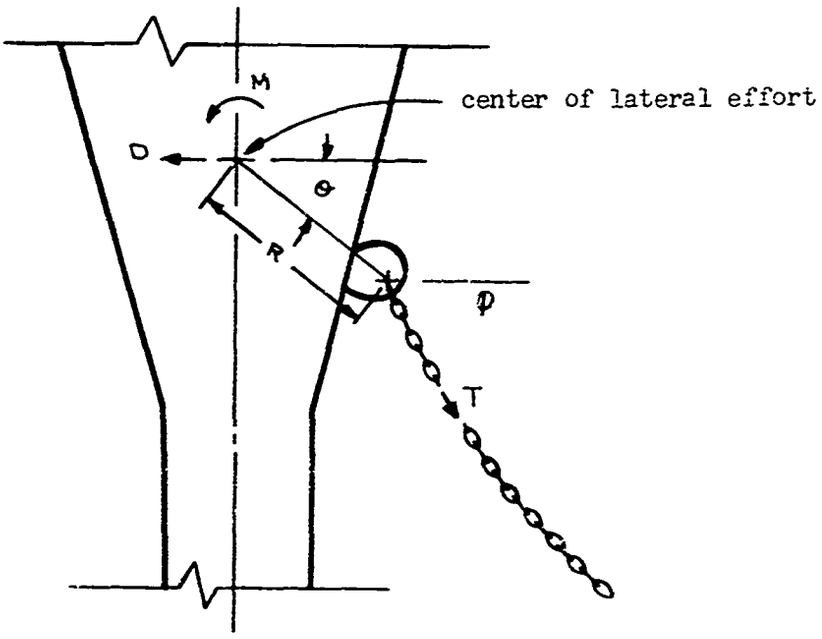

We shall assume that the chain is not very taut. In other words, that at least some portion of the chain lies along the bottom. This assumption is appropriate for low to moderate currents. Under these conditions, the chain tension is given by

$$T = \frac{zw}{1-\cos\phi} \qquad (1)$$

where

z = distance of the mooring point off the bottom

w = the weight of the chain per foot

We also assume that the total drag, D, of the buoy acts through one point on the buoy centerline. The total moment, M, of the forces

about the center of lateral effort is given by

$$M = -\frac{z\,wR\sin(\phi-\theta)}{1-\cos\phi} + M_o \qquad (2)$$

where

R & θ are defined in the above figure.

M_o is the moment caused by the counterweight.

If M_o is chosen so that M = 0 when $\phi = 90^\circ$ (corresponding to D=0), then (2) becomes

$$M = z\,w\,R\left\{\cos\phi - \frac{\sin(\phi-\theta)}{1-\cos\phi}\right\}$$

or

$$\bar{M} = \frac{M}{zwR} = \left\{\frac{\cos\phi\sin\theta-(\sin\phi+\cos\phi-1)\cos\theta}{(1-\cos\phi)}\right\} \qquad (3)$$

Further, the horizontal component of the chain force must equal the drag. Thus,

$$D = zw\left\{\frac{\cos\phi}{1-\cos\phi}\right\}$$

or

$$\bar{D} = \frac{D}{zw} = \left\{\frac{\cos\phi}{1-\cos\phi}\right\} \qquad (4)$$

For each value of the non-dimensional parameter $\bar{D}$, we can determine φ from (4). This value of φ can be used to determine the non-dimensional moment, $\bar{M}$, from (3). Figure C-1 shows the variation of $\bar{M}$ with $\bar{D}$ for various angles θ.

It can be seen that for moderate values of D that an angle, θ, near 35° produces a near-zero $\bar{M}$. It is to be noted that if the product (zw)

remains constant then $\bar{D}$ is just a function of the drag of the buoy (i.e., a function of current only). In this case the buoy pitch characteristics are a function of current only and not of the depth, z. Further, the required counterweight moment, M_o, is also independent of depth.

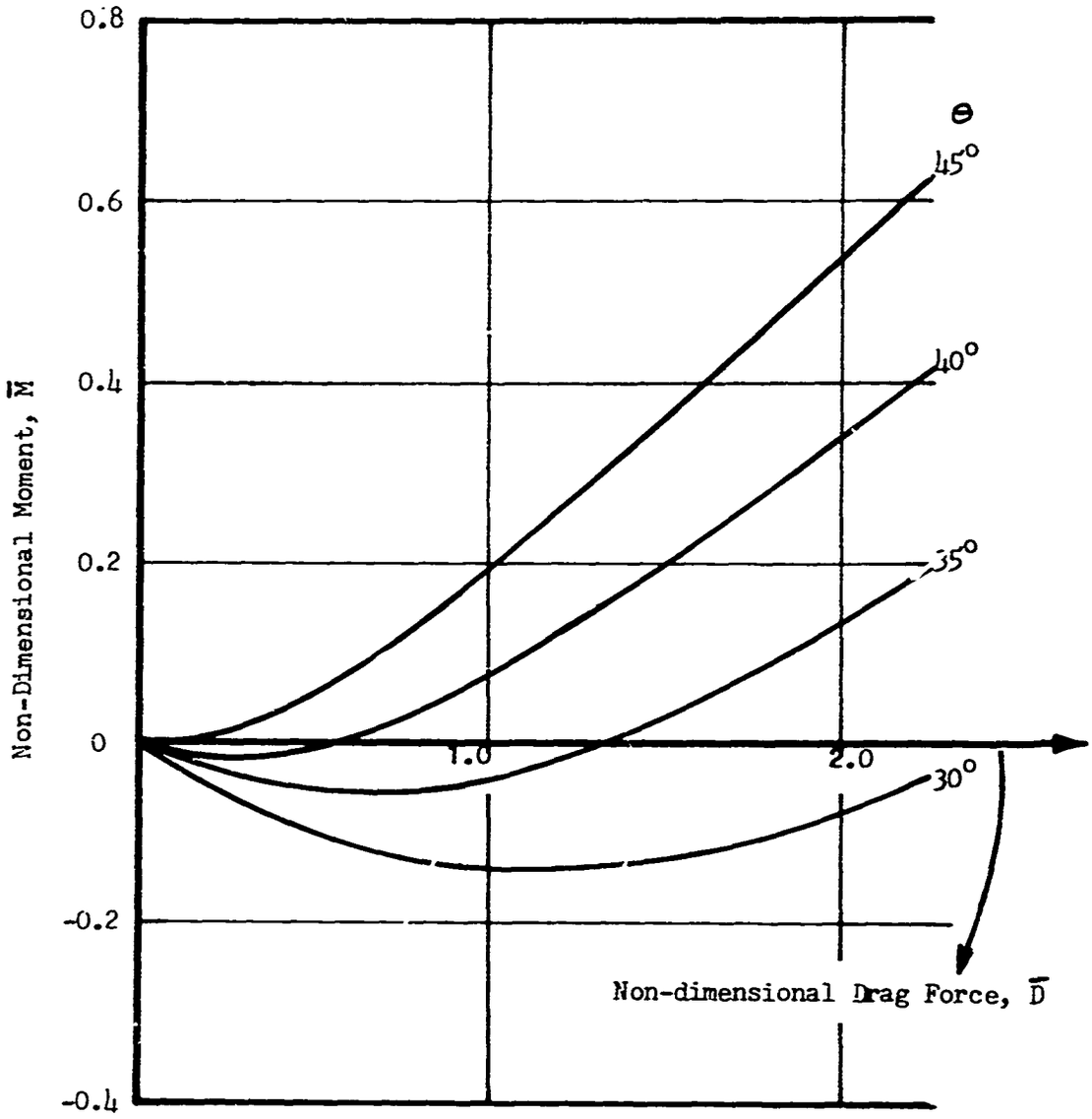

Figure C-1. Variation of $\bar{M}$ with $\bar{D}$ for Various Values of Θ.

Lockheed
MISSILES
& SPACE
COMPANY

24 March 1969

Mr. Robert Kuehn
Signal Branch, U.S. Coast Guard
Station 2-12
Washington, D. C. 20591

Dear Bob:

I looked up the natural frequency information you asked Bob Waid for and listed these figures in the table below. Since I also had the damping factors for these runs I have included them too.

Buoy	Period	Damping Factor
1 CR	7.0 sec	0.14
8x26	5.6 sec	0.08
CANUN	5.2 sec	0.10
CANUN II	5.8 sec	0.05
CANUN IIa	5.2 sec	0.16

The periods refer to the full scale buoy.

If you have any further questions do not hesitate to call.

Sincerely,

LOCKHEED MISSILES & SPACE COMPANY

Bill Webster

W. C. Webster
Hydrodynamics,
Ocean Systems

WCW/amw

UNCLASSIFIED

DOCUMENT CONTROL DATA - R & D

Security classification of title, body of abstract and indexing annotation must be entered when the overall report is classified

1. ORIGINATING ACTIVITY (Corporate author)
Lockheed Missiles and Space Company
Underwater Missile Facility
Sunnyvale, California

2a. REPORT SECURITY CLASSIFICATION
Unclassified

2b. GROUP

3. REPORT TITLE
AN EXPERIMENTAL STUDY TO DETERMINE THE MOTIONS AND MOORING TENSIONS OF THREE BUOYS.

4. DESCRIPTIVE NOTES (Type of report and inclusive dates)
Final Technical Report

5. AUTHOR(S) (First name, middle initial, last name)
Dr. William C. Webster

6. REPORT DATE	7a. TOTAL NO. OF PAGES	7b. NO OF REFS
27 December 1968	87	None

8a. CONTRACT OR GRANT NO	9a. ORIGINATOR'S REPORT NUMBER(S)
DOT-CG-83851A b. PROJECT NO LMSC/D022460 c. d.	9b. OTHER REPORT NO(S) (Any other numbers that may be assigned this report)

10. DISTRIBUTION STATEMENT
Statement No. 1; Distribution of this document is unlimited.

11. SUPPLEMENTARY NOTES	12. SPONSORING MILITARY ACTIVITY
	U. S. Coast Guard Ocean Engineering Division 400 7th St. N.W. Washington, D.C.

13. ABSTRACT

This experimental program was aimed at determing the attitude, the motions, and the mooring tensions of three types of buoys in representative ranges of currents and ocean waves. The first two buoy types, called the 1CR and 8x26LR, represent two common types now in use by the Coast Guard. The third type tested was the CANUN, a new filament wound fiberglass buoy currently under development. The objective of the study was to determine not only the relative merits of these buoys but to determine the absolute effect of these motions on the visibility of the buoy under realistic sea conditions.

DD FORM 1 NOV 68 1473

UNCLASSIFIED
Security Classification

UNCLASSIFIED
Security Classification

14. KEY WORDS	LINK A		LINK B		LINK C	
	ROLE	WT	ROLE	WT	ROLE	WT
DESCRIPTIONS: (*BUOYS, MOTION AND MOORING TENSIONS), HEAVE, PITCH, ROLL, SWAY, SURGE, (TEST FACILITIES AND INSTRUMENTATION). LOCKHEED UNDERWATER MISSILE FACILITY, DISPLACEMENT PROBE, GYRO, LOAD CELL, WAVE GAUGE, (*GYRADIUS ANALYSIS), (*MOORING, SINGLE POINT)						

UNCLASSIFIED
Security Classification